8-27-2009

Magma Extraction from the Mantle Wedge at Convergent Margins Through Dikes: A Parametric Sensitivity Analysis

Scott E. Johnson
University of Maine - Main, johnsons@maine.edu

Z.-H. Jin

Geochemistry Geophysics Geosystems G3
AN ELECTRONIC JOURNAL OF THE EARTH SCIENCES
Published by AGU and the Geochemical Society

Article
Volume 10, Number 8
27 August 2009
Q08017, doi:10.1029/2009GC002419
ISSN: 1525-2027

Magma extraction from the mantle wedge at convergent margins through dikes: A parametric sensitivity analysis

S. E. Johnson
Department of Earth Sciences, University of Maine, Orono, Maine 04469, USA (johnsons@maine.edu)

Z.-H. Jin
Department of Mechanical Engineering, University of Maine, Orono, Maine 04469, USA (zhihe.jin@maine.edu)

[1] We address under what conditions a magma generated by partial melting at 100 km depth in the mantle wedge above a subduction zone can reach the crust in dikes before stalling. We also address under what conditions primitive basaltic magma (Mg # > 60) can be delivered from this depth to the crust. We employ linear elastic fracture mechanics with magma solidification theory and perform a parametric sensitivity analysis. All dikes are initiated at a depth of 100 km in the thermal core of the wedge, and the Moho is fixed at 35 km depth. We consider a range of melt solidus temperatures (800–1100°C), viscosities (10–100 Pa s), and densities (2400–2700 kg m^{-3}). We also consider a range of host rock fracture toughness values (50–300 MPa $m^{1/2}$) and dike lengths (2–5 km) and two thermal structures for the mantle wedge (1260 and 1400°C at 100 km depth and 760 and 900°C at 35 km depth). For the given parameter space, many dikes can reach the Moho in less than a few hundred hours, well within the time constraints provided by U series isotope disequilibria studies. Increasing the temperature in the mantle wedge, or increasing the dike length, allows additional dikes to propagate to the Moho. We conclude that some dikes with vertical lengths near their critical lengths and relatively high solidus temperatures will stall in the mantle before reaching the Moho, and these may be returned by corner flow to depths where they can melt under hydrous conditions. Thus, a chemical signature in arc lavas suggesting partial melting of slab basalts may be partly influenced by these recycled dikes. Alternatively, dikes with lengths well above their critical lengths can easily deliver primitive magmas to the crust, particularly if the mantle wedge is relatively hot. Dike transport remains a viable primary mechanism of magma ascent in convergent tectonic settings, but the potential for less rapid mechanisms making an important contribution increases as the mantle temperature at the Moho approaches the solidus temperature of the magma.

Components: 13,608 words, 16 figures.

Keywords: magma dynamics; mantle wedge; dike propagation; channelized magma transport.

Index Terms: 8434 Volcanology: Magma migration and fragmentation; 8020 Structural Geology: Mechanics, theory, and modeling; 0545 Computational Geophysics: Modeling (4255).

Received 2 February 2009; **Revised** 12 May 2009; **Accepted** 6 July 2009; **Published** 27 August 2009.

Johnson, S. E., and Z.-H. Jin (2009), Magma extraction from the mantle wedge at convergent margins through dikes: A parametric sensitivity analysis, *Geochem. Geophys. Geosyst.*, *10*, Q08017, doi:10.1029/2009GC002419.

1. Introduction

[2] Growth or removal of continental crust occurs by a number of processes working separately or together, including arc magmatism, intraplate volcanism, oceanic plateau accretion, crustal underplating, ophiolite accretion, arc surface erosion, sediment subduction, tectonic erosion and delamination. In a review and reappraisal of geophysical data for western Pacific island arcs, *Dimalanta et al.* [2002] concluded that arc magmatism is a primary mechanism for continental crustal growth in these arcs, adding 30–95 km^3/km/Ma. The importance of arc magmatism in the formation of continental crust raises long-standing questions of how and where melting occurs in the subarc mantle wedge, how this melt segregates into batches large enough to ascend, and what mechanisms facilitate ascent. This paper is concerned with ascent, and in particular we assess the effectiveness of dikes in transporting segregated magma batches in short time frames from the core of a mantle wedge at 100 km depth to the subarc Moho at 35 km depth. Few efforts [e.g., *Carmichael et al.*, 1977; *Spera*, 1980, 1984, 1987; *Dahm*, 2000a] have been made to explore the time and length scales involved in this process, which requires a coupled thermal-mechanical approach. Nevertheless, we believe it is an important issue to pursue because of (1) the geochemical evidence for primitive (Mg # > 60) mantle-derived magmas in arc crust [e.g., *Kelemen et al.*, 2003a]; (2) the common occurrence of dikes in these arcs, including dikes with primitive magma compositions [e.g., *Leat et al.*, 2002]; (3) the role of mantle-derived basaltic magma in generating felsic melts through partial melting of crustal rocks [e.g., *Dufek and Bergantz*, 2005]; and (4) the mechanical efficiency with which dikes can transport magma across large distances in short times [e.g., *Rubin*, 1995a].

[3] During subduction, hydrous fluids are released from downgoing slabs by dehydration reactions, and these fluids enter the overlying mantle wedge [e.g., *Schmidt and Poli*, 2003]. The presence of fluids lowers the solidus of mantle peridotite, and it is generally thought that magmatism in convergent margins is caused primarily by fluid-induced partial melting of the mantle wedge [e.g., *Gill*, 1981; *Tatsumi*, 1989; *Kushiro*, 1990; *Davies and Bickle*, 1991; *Davies and Stevenson*, 1992; *Arculus*, 1994; *Grove et al.*, 2006]. This process typically generates basaltic magmas, but *Kelemen et al.* [2003a] have reviewed arguments that primitive andesites may also form by interaction between mantle peridotite and partial melt of subducted eclogite-facies metabasalts or metasediments.

[4] Though fluid-induced melting is the prevailing view, numerous studies have argued for a component of decompression melting in the production of arc lavas [e.g., *Plank and Langmuir*, 1988; *Pearce and Parkinson*, 1993; *Sisson and Bronto*, 1998; *Elkins-Tanton et al.*, 2001; *Cameron et al.*, 2003], and some component of decompression melting appears plausible given the upwelling flow in the mantle wedge predicted by models that incorporate temperature-dependent mantle viscosity [e.g., *Furukawa*, 1993; *Eberle et al.*, 2002; *van Keken et al.*, 2002; *Kelemen et al.*, 2003a, 2003b; *Conder*, 2005; *Manea et al.*, 2005a, 2005b; *Peacock et al.*, 2005]. Fluid-induced and decompression melting can produce magmas with a wide range of water content, which will affect magma solidus temperatures, viscosities and densities [e.g., *Spera*, 2000; *Gaetani and Grove*, 2003]. These are important variables in assessing whether or not magma formed in the mantle at depths of ~100 km can travel the distance required to reach the base of the continental crust before solidifying. Our parametric sensitivity analysis below is aimed partly at assessing the effects of these variables on dike propagation velocities and distances.

1.1. Background Considerations

1.1.1. Constraints on Magma Transport Rates in the Mantle

[5] Isotopic disequilibria studies over the past decade using ^{238}U-^{230}Th (^{230}Th half-life 75.4 ka), ^{235}U-^{231}Pa (^{231}Pa half-life 32.8 ka), and ^{226}Ra-^{230}Th (^{226}Ra half-life 1.6 ka) isotopic systems provide important constraints on magma transport times at convergent margins, indicating that partial melts of the mantle must move rapidly from the mantle wedge source, through the lithosphere, at an average rate on the order of 1 km a^{-1} [*Turner et al.*, 2000, 2001, 2003; *Bourdon et al.*, 2003; *Peate and Hawkesworth*, 2005]. Such rapid transport times require channelized flow, and currently there are two options: magma-filled fractures [e.g., *Nicolas*, 1990; *Rubin*, 1995a, 1998; *Kuhn and Dahm*, 2004] and porous flow via "reaction infiltration instabilities" [e.g., *Aharonov et al.*, 1995; *Kelemen et al.*, 1997; *Spiegelman and Kelemen*, 2003; *Stracke et al.*, 2006]. Channeling of flow by reaction infiltration instabilities has been proposed for melt extraction through permeable dunite channels in divergent margin settings. Given

very low melt viscosity and density, very small mantle grain size, and high permeability, these channels may be able to transport melt at rates up to 100 m a^{-1} [*Kelemen et al.*, 1997, 2003a; *Spiegelman and Kelemen*, 2003; *Stracke et al.*, 2006]. This is fast enough to transport magma from 100 km depth to the crust in less than the half-life of ^{226}Ra (1.6 ka), which suggests that current isotopic disequilibria constraints cannot be used to explicitly discriminate between dike transport and porous flow.

[6] The propagation distance attainable by porous flow is strongly dependent on the thermal structure of the mantle. Some arcs appear to be underlain by transiently hot mantle [e.g., *Elkins-Tanton et al.*, 2001], so a hydrous partial melt might be able to traverse the mantle by porous flow without freezing. In cooler arcs, where the temperature of the subarc mantle lies below the solidus of the migrating melt, transport rates must be high enough to avoid stalling (dikes) or freezing (porous flow) caused by solidification. Dikes can transport basaltic melt at rates on the order of kilometers per day [e.g., *Spence et al.*, 1987; *Lister and Kerr*, 1991; *Rubin*, 1995a; *Dahm*, 2000b; *Jin and Johnson*, 2008a], which means that they will have less difficulty transporting hot, primitive magmas across a thick thermal boundary layer. Diking and porous flow need not act separately. For example, in some instances there may be a transition from porous flow to melt-filled fracture propagation in the upper part of the mantle, as proposed for mid-ocean ridges [e.g., *Kelemen et al.*, 1997]. Nevertheless, dike propagation from the deeper mantle is not precluded on mechanical or chemical grounds, and the efficiency and mathematical tractability of dikes invites careful analysis and consideration.

1.1.2. Effects of Magma Solidification During Dike Propagation

[7] With rare exceptions [e.g., *Spera*, 1980; *Carrigan et al.*, 1992], magma flow in dikes is treated as laminar flow. Under such conditions, magma traveling in dikes through a host that is cooler than the magma solidus temperature will solidify against the dike walls at a rate determined by the thermal gradient. This solidification reduces the magma volume, and therefore the buoyancy force driving the flow, leading to reduced dike propagation velocity and distance. Eventually, with continued solidification, the dike will reach its critical length and stall. This does not mean that the dike has frozen solid, but rather that the magma volume is no longer large enough to provide the required buoyancy force to propagate critically. *Carrigan et al.* [1992] have shown that the onset of magma solidification along a dike wall can be significantly delayed if even a minor cross-stream flow occurs in the dike. Given the roughness of typical dike walls exposed at Earth's surface, we expect some divergence from laminar flow to be common. Therefore, the solidification rates that we calculate in our analysis may be on the high side when the magma temperature is well above the solidus temperature.

[8] There are two contributions to the thermal effect; the change in background temperature with depth and the change in magma solidus with depth. *Delaney and Pollard* [1982], *Bruce and Huppert* [1990], *Lister and Dellar* [1996], and *Fialko and Rubin* [1998] studied magma solidification in dikes, but they assumed that the dike walls were rigid and therefore did not incorporate elastic deformation of the walls. Incorporating elastic dike wall deformation is critical for modeling the propagation of a dike with an advancing, closed tail owing to the required nonplanar wall geometry. *Lister* [1994a, 1994b] did include elastic deformation of the dike walls during cooling, and derived solutions of dike propagation under both constant volume release and continual release conditions at the dike base. *Bolchover and Lister* [1999] developed a three-dimensional model for a dike propagating laterally along the level of neutral buoyancy and discussed the effect of fracture toughness on magma solidification and hence dike propagation. The above studies effectively assumed that (1) magma remains at its solidification temperature during dike propagation, (2) dikes are connected to a magma chamber or source region and therefore are driven by both magma buoyancy and the source overpressure, and (3) the host rock is at a constant temperature. The effect of excess magma temperature above the solidification temperature, which increases the distance a dike can propagate before arresting, was included in the study of *Rubin* [1995b].

1.1.3. Effects of Dike Interaction During Transport

[9] Elastic interaction of simultaneously propagating dikes can have a profound effect on dike propagation distances and patterns. Because dikes elastically deform the surrounding material, dike interaction can lead to smaller opening widths, leading to reduced velocities and fluxes [e.g., *Jin*

and Johnson, 2008a]. The interactions among the stress fields produced by individual dikes can lead to repulsion or coalescence [e.g., *Takada*, 1994; *Ito and Martel*, 2002] and in the case of coalescence the development of a characteristic spacing for the resulting larger dikes [e.g., *Ito and Martel*, 2002]. The simultaneous effects of coupling magma solidification and simultaneous propagation of multiple dikes have not been considered in previous publication that we are aware of. We include a subset of those effects here, in addition to our analysis of single dikes.

1.1.4. Effects of Melting History, Water Content, Melt Viscosity, Melt Density, and Solidus Temperatures on Melt Segregation and Transport Rates

[10] Melting history, and the water content, solidus temperature, viscosity and density variation of melt in the mantle wedge are all important considerations in evaluating models for melt segregation and ascent, but all are relatively poorly understood. *Grove et al.* [2006] suggest that melt percentages could be as high as 15% in the hot core of the mantle wedge. They also suggest that H_2O content in partial melts of the wedge could range from 28% near the slab interface to less than 5% in the thermal core. Such a range in H_2O content would have profound effects on melt density, viscosity and connectivity. *Gaetani and Grove* [2003] have reviewed these effects, calculating that melt density may decrease by $\sim$50 kg/m^3 per wt % H_2O, and melt viscosity may decrease by $\sim$0.25 Pa s per wt % H_2O [see also *Spera*, 2000]. They also reviewed the literature on melt-solid dihedral angles in static peridotite melting experiments, finding that the presence of H_2O is likely to increase melt interconnectivity in partial molten peridotite. Significant melt percentages in the mantle wedge combined with lowered viscosities, densities and dihedral angles that come with H_2O make the likelihood of segregation high, particularly given the volumetric and shear strain rate gradients in the wedge. Recent experimental work [*Katz et al.*, 2006; *Holtzman and Kohlstedt*, 2007] has shown that magma may segregate into bands oriented at 15–25° to the shear plane during approximately simple shear deformation of partially molten rock. Scaling from the experiments suggest that fluid pressure differences between the melt-rich bands and less melt-rich matrix on the order of 1 MPa are likely. Under asthenospheric mantle conditions, this is a high enough fluid pressure gradient to drive segregation over spatial scales and compaction lengths consistent with dunite channel spacing preserved in ophiolites. This work may provide a mechanism for generating the long, narrow, magma-rich bands that could feed or develop into dikes.

[11] The solidus temperatures of peridotite and resulting basaltic melt play an important role in determining the maximum possible propagation distance of a dike. A range of water saturated peridotite solidi have been produced in melting experiments, as reviewed by *Grove et al.* [2006]. In addition, a range of basalt solidi are available for variably saturated conditions [e.g., *Liu et al.*, 1996; *Schmidt and Poli*, 1998].

1.2. Boundary Conditions

[12] To establish the boundary conditions for our analyses, we consider two generalized thermal structures in the mantle at a convergent margin where oceanic lithosphere is subducting beneath continental lithosphere (Figure 1). These thermal structures reflect temperature-dependent viscous mantle rheology, which allows hot mantle undergoing corner flow in the wedge to reach significantly closer to the surface than models that consider isoviscous mantle. This higher reach of hotter mantle also leads to higher temperatures at the slab/mantle interface, where fluid saturated sediments at the top of the slab may melt [e.g., *Schmidt and Poli*, 2003]. Figure 1a [after *Manea et al.*, 2005a] shows a relatively conservative thermal structure, in which the core of the mantle wedge at 100 km depth is $\sim$1260°C, and the temperature at the Moho is $\sim$760°C. Petrological evidence [e.g., *Kelemen et al.*, 2003a, 2003b] and some numerical experiments [e.g., *Furukawa*, 1993; *van Keken et al.*, 2002; *Kelemen et al.*, 2003b; *Conder*, 2005] suggest that temperatures in the mantle wedge may be significantly higher than those depicted in Figure 1a, and so we also evaluate a thermal structure similar to that depicted in Figure 1b [after *van Keken et al.*, 2002] in which the core of the mantle wedge at 100 km depth is $\sim$1400°C, and the temperature at the Moho is $\sim$900°C. Exact temperature distributions are model-dependent, and our methodology is not affected by these differences, but the thermal structure plays a large role in determining whether or not dikes with vertical dimension near their critical length make it to the crust/mantle boundary, as we show in our analyses below.

1.3. Objectives of the Present Study

[13] Our purpose here is to place some mechanical constraints on the ascent of partial melts from the

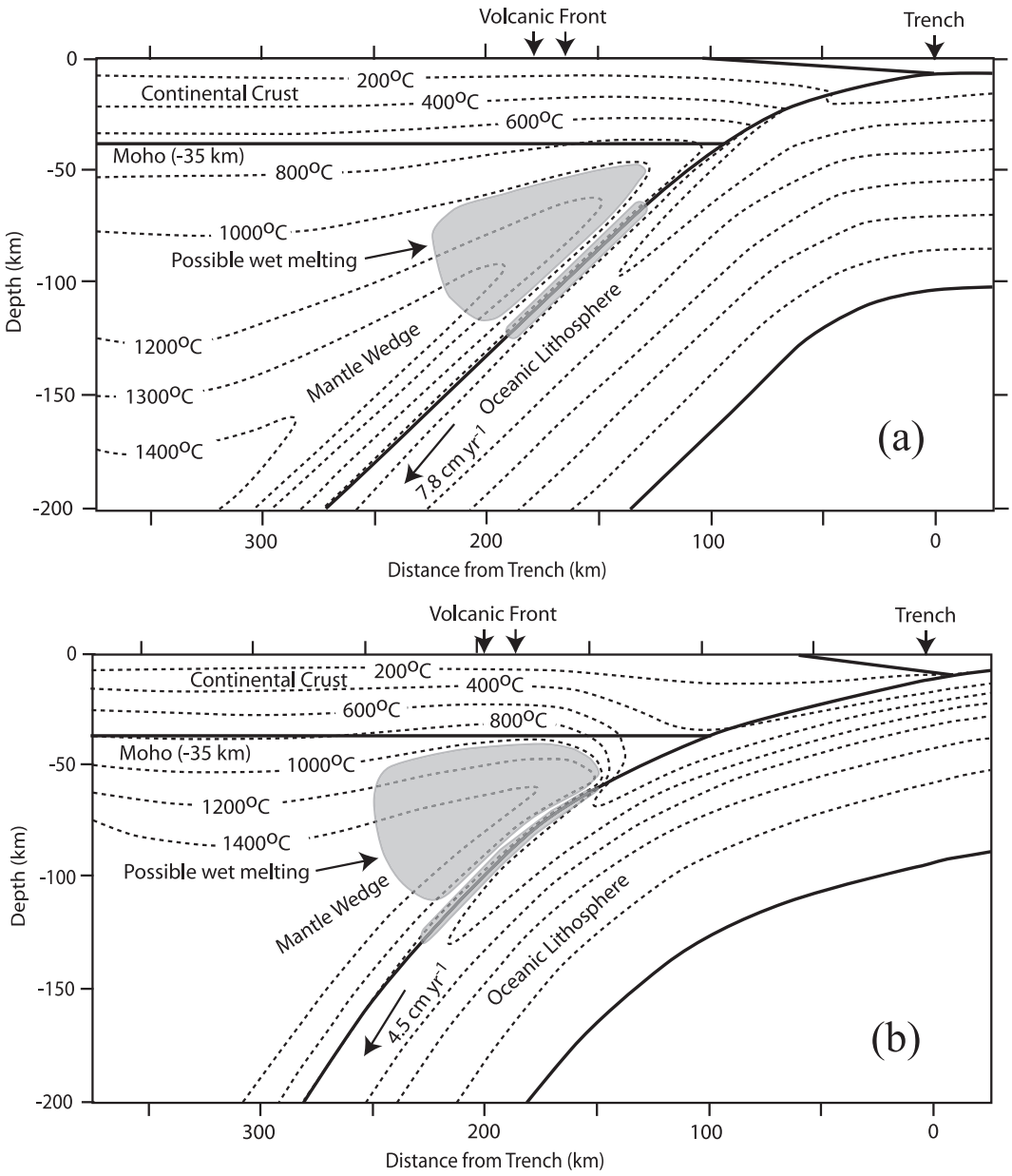

Figure 1. Generalized thermal fields for subduction at a continental-oceanic convergent margin. (a) Relatively cool mantle wedge (modified from *Manea et al.* [2005a]). The mantle has a temperature-dependent viscosity, which results in a portion of the mantle wedge below the arc lying within the wet peridotite melting field. The shaded area in the mantle wedge shows potential regions of both hydration melting from the release of slab fluids and decompression melting caused by the temperature-dependent mantle rheology. The shaded region at the top of the slab shows where slab melting of sediments or basaltic crust may occur. Shaded regions after *Wiens et al.* [2008]. (b) Relatively hot mantle wedge (modified from *van Keken et al.* [2002]). The mantle has a stress and temperature-dependent viscosity. Shading as in Figure 1a.

mantle wedge to the crust by calculating the propagation distances of dikes filled with magma that have a range of solidus temperatures and physical properties. The central questions to be addressed are, under what circumstances can partial melts produced in the mantle reach the crust in dikes before they stall because of marginal chilling and length reduction, and what affect does dike interaction have on propagation distance? We assume that dike propagation is driven by magma buoyancy with no contribution from source overpressure as assumed in some other studies. We also assume that the host rock is linearly elastic, and where more than one dike is propagating we

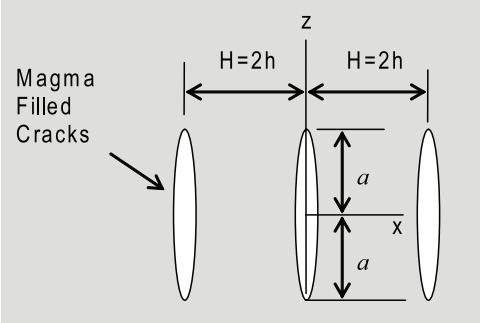

Figure 2. An array of periodic parallel dikes in z (vertical) direction.

assume that the dikes are parallel and have equal length. Although parts of the mantle may not respond as a linear elastic solid, particularly where partial melts are present, we apply this assumption as an end-member with the intention of including the effects of viscoplastic energy dissipation in a later analysis. We further assume that simultaneously propagating dikes are periodically distributed so that a two-dimensional, semianalytical approach becomes applicable.

[14] Numerical results are presented to quantitatively illustrate the effects of dike interactions and magma solidification on the propagation distance, and to determine whether or not specific dikes will make it to the crust/mantle boundary for a given mantle thermal structure. In order to reduce our primary sensitivity analysis to some reasonable parameter space, we assume that they initiate near the thermal core of the mantle wedge at 100 km depth, that the magma in the dikes starts off at the local wedge temperature of 1260°C or 1400°C at ~100 km depth (Figures 1a and 1b), and that the temperature at the crust/mantle boundary is either 760°C or 900°C at 35 km depth (Figures 1a and 1b). For our initial analyses in which we include dike propagation velocity against time, we assume that all dikes have a vertical length of 2 km. This assumption allows us to evaluate the relatively sensitive parameter space in which some dikes make it to the crust, whereas others do not. We conduct sensitivity around melt solidus temperature, melt density, melt viscosity and host rock fracture toughness. Our results indicate that many dikes of 2 km length will not make it to the crust/mantle boundary. We therefore evaluate the effect of increasing dike length up to 5 km and calculate the normalized volume change of dikes of various length from depth of initiation to the Moho. This calculation allows us to place some constraints on dikes that are capable of transporting magmas with primitive composition to the crust.

2. Multiple Dike Propagation With Magma Solidification: Formulations

2.1. Fracture Mechanics of Dike Propagation

[15] We consider vertical, buoyancy-driven propagation of both single dikes, and an array of parallel dikes, as shown in Figure 2, where $2a$ is the length of the dikes in the vertical direction and $H = 2h$ is the dike spacing (mathematically, single dikes correspond to an infinite spacing, i.e., $h/a \rightarrow \infty$). We assume that the size of these dikes in the perpendicular direction to the x-z plane is large so that a two-dimensional, plane strain model can be used. Figure 2 thus shows a vertical section through these "blade" dikes in the x-z plane with the lower and upper dike tips at $z = -a$ and $z = a$, respectively.

[16] In a mantle wedge setting, propagation paths of dikes may be influenced by buoyancy forces, stress gradients arising from variations in the topographic load, and the stress field arising from subduction-induced mantle flow, which is sensitive to the velocity and angle of subduction and the position in the wedge from which the dikes originate [e.g., *Furukawa*, 1993; *Dahm*, 2000a]. Both *Furukawa* [1993] and *Dahm* [2000a] calculated the stress fields in a mantle wedge and estimated the magma migration paths that would be followed by dikes. The stress fields calculated in these two studies are broadly similar, and *Furukawa* [1993] suggested that dikes would follow a curved path tracking the maximum compressive stress that would naturally lead to migration toward the base of the volcanic arc. *Dahm* [2000a] found similar results, but also showed that longer dikes possess enough buoyancy to propagate in a more vertical direction that deviates from the principal stress orientations. In general we conclude that dikes originating from 100 km depth, approximately below the volcanic arc, as considered here, will propagate upward toward the arc in a path that could be curved. Calculated stress orientations are model-dependent, so we consider our assumption of vertical dike propagation to be reasonable for the purposes of our analysis, noting that a curved path would increase the distance that would need to be traversed to reach the Moho.

[17] Because dike propagation velocities (on the order of 1 m/s or smaller) are much smaller than

the wave speed of the host rocks, the inertial effects can be ignored and the problem becomes quasi-static. We use a singular integral equation method to analyze the dike propagation problem. The formulations described in this section follow those given by *Jin and Johnson* [2008b]. Although the theoretical model applicable to the case of multiple dikes is for an infinite array of parallel dikes, the results are approximately valid for central dikes in a finite array. The basic integral equation has the following form

$$\int_{-1}^{1}\left[\frac{1}{s-r}+ak(r,s)\right]\frac{\psi(s)}{\sqrt{1-r^2}}ds=-\frac{2\pi(1-\nu^2)}{E}p_{net}(r),\quad |r|\le 1 \tag{1}$$

where E is Young's modulus, ν Poisson's ratio, $r = z/a$, $\psi(z)$ the unknown density function

$$\psi(z)/\sqrt{1-(z/a)^2}=\varphi(z)=(\partial u_x/\partial z)|_{x=0} \tag{2}$$

with $u_x(z, x)$ being the displacement perpendicular to the dikes, $ak(z, z')$ a known Fredholm kernel depending on the dike spacing to length ratio h/a, and $p_{net}(z)$ is the net (or excess) pressure on the dike surfaces due to magma buoyancy, magma flow within the dikes, confining pressure and tectonic stresses.

[18] In general, problems of magma flow and dike propagation are coupled together so that the magma pressure, stress field, dike surface profile and dike propagation velocity interact with each other and must be determined simultaneously. However, for slow dike propagation (on the order of 1 m/s or less) a simplified approach used by *Weertman* [1971] and *Nunn* [1996] may be employed. In this simplified approach, the net pressure, p_{net}, on the dike surface is described by a linear function

$$p_{net}(z)=p_0(t)+p_1(t)z \tag{3}$$

where t is time, p_0 is the net pressure at the dike center ($z = 0$), and p_1 is the net pressure gradient. In equation (3), p_0 and p_1 are determined using a fracture mechanics criterion at the dike tips.

[19] With the dike surface net pressure given by a linear function in equation (3), the unknown function ψ (r) of the integral equation (1) may be expressed in the following normalized form

$$\psi(r)=\frac{1-\nu^2}{E}\left[p_0\tilde{\psi}^{(0)}(r)+p_1a\tilde{\psi}^{(1)}(r)\right] \tag{4}$$

Once the solution of the integral equation is obtained, the stress intensity factors at the upper and lower dike tips can be calculated from

$$K_I(a)=-\frac{1}{2}\sqrt{\pi a}\left[p_0\tilde{\psi}^{(0)}(1)+p_1a\tilde{\psi}^{(1)}(1)\right],$$
$$K_I(-a)=\frac{1}{2}\sqrt{\pi a}\left[p_0\tilde{\psi}^{(0)}(-1)+p_1a\tilde{\psi}^{(1)}(-1)\right] \tag{5}$$

The dike surface opening displacement (dike thickness) can be calculated from

$$\delta(r)=-\frac{2a(1-\nu^2)}{E}\left[p_0\int_r^1\frac{\tilde{\psi}^{(0)}(s)}{\sqrt{1-s^2}}ds+p_1a\cdot\int_r^1\frac{\tilde{\psi}^{(1)}(s)}{\sqrt{1-s^2}}ds\right] \tag{6}$$

[20] The stress intensity factor at the upper dike tip equals the fracture toughness during dike propagation. At the same time we assume that the lower dike tip closes. In fracture mechanics, these conditions are described by

$$K_I(a)=K_{Ic},\quad K_I(-a)=0 \tag{7}$$

where K_{Ic} the fracture toughness of the host rock. Substituting equation (5) into equation (7), solving the resulting equations for p_0 and p_1, and considering symmetry conditions for $\tilde{\psi}^{(0)}(r)$ and $\tilde{\psi}^{(1)}(r)$, we have

$$p_0=-\frac{K_{Ic}}{\sqrt{\pi a}\,\tilde{\psi}^{(0)}(1)},\quad p_1=-\frac{K_{Ic}}{a\sqrt{\pi a}\,\tilde{\psi}^{(1)}(1)} \tag{8}$$

Because dike length changes during propagation, p_0 and p_1 become functions of time. The above formulation also assumes simultaneous propagation of the parallel dikes. Although difficult to demonstrate in nature, simultaneous growth of parallel cracks is soundly rooted in the physics of materials. For example, simultaneous parallel crack growth is common in ceramics and glasses when subjected to thermal gradients [*Gupta*, 1972; *Bahr et al.*, 1986]. In addition, dike growth simlation experiments using gelatin and silicone showed simultaneous nucleation and growth of dikes around the margins of a pressured chamber [*Canon-Tapia and Merle*, 2006]. Given the volumes of magma extracted from the mantle wedge we consider it likely that multiple dike propagation events will occur periodically throughout the subduction process, but our single-dike solutions are otherwise applicable.

2.2. Dike Propagation Velocity

[21] Magma flow in the dikes can be described by the lubrication theory. Following *Nunn* [1996], the dike propagation velocity, V, is approximately determined using the relationship of Poiseuille flow as follows

$$V = \frac{\delta_{ave}^2}{12\eta}(\Delta\rho g - p_1) = \frac{\delta_{ave}^2}{12\eta}\left(\Delta\rho g + \frac{K_{Ic}}{a\sqrt{\pi\, a}\;\widetilde{\psi}^{(1)}(1)}\right) \quad (9)$$

where δ_{ave} is the average separation of the two dike surfaces defined by

$$\delta_{ave} = \frac{1}{2a}\int_{-a}^{a}\delta(z)dz = -\frac{(1-\nu^2)a}{E} \cdot \int_{-1}^{1}\left[p_0\int_{r}^{1}\frac{\widetilde{\psi}^{(0)}(s)}{\sqrt{1-s^2}}ds + p_1 a\int_{r}^{1}\frac{\widetilde{\psi}^{(1)}(s)}{\sqrt{1-s^2}}ds\right]dr \quad (10)$$

η the magma viscosity, g the gravitational acceleration, $\Delta\rho = \rho_r - \rho_m$, ρ_r the rock density, ρ_m the magma density, and p_0 and p_1 given in equation (8).

2.3. Magma Solidification

[22] As dikes propagate through host rock that is cooler than the magma solidus, the magma within the dikes solidifies against the dike surfaces. Assuming laminar flow, the thickness, b, of the solidified layer is given by [*Turcotte and Schubert*, 2002]

$$b = 2\lambda\sqrt{\kappa\Delta t} \quad (11)$$

where κ is the thermal diffusivity, Δt the time since the magma came in contact with the host rock, and λ a function of a number of parameters including the specific heat c, the latent heat of solidification L, the solidification temperature T_s, the magma temperature T_m, and the remote rock temperature T_0. When the magma temperature equals the solidification temperature, λ is determined by the following equation [*Turcotte and Schubert*, 2002]

$$\lambda\exp(\lambda^2)(1 + erf(\lambda)) = \frac{c(T_s - T_0)}{L\sqrt{\pi}} \quad (12a)$$

where erf() is the error function. When the magma temperature is higher than the solidification temperature, λ satisfies the following equation [*Rubin*, 1995b]

$$\lambda\exp(\lambda^2) = \frac{c}{L\sqrt{\pi}}\left[\frac{T_m - T_0}{1 + erf(\lambda)} - \frac{T_m - T_s}{1 - erf(\lambda)}\right] \quad (12b)$$

We note that T_0 is not a constant and decreases following the geothermal gradient during vertical propagation of the dikes. As mentioned above, a small component of cross-stream flow in the dike owing for example to dike wall roughness will provide effective thermal mixing and strongly retard dike wall solidification [e.g., *Carrigan et al.*, 1992]. Our estimates below for dike propagation distance assume laminar flow, and are therefore conservative.

2.4. Dike Propagation Distance

[23] Consider dike propagation from time t_i to t_{i+1} (i = 0, 1, 2, . . ., I). The propagation distance during the period is denoted by Δd_i, which is related to $t_{i+1} - t_i$ by

$$\Delta d_i = V_i(t_{i+1} - t_i) = \frac{\left(\delta_{ave}^i\right)^2}{12\eta}(\Delta\rho g - p_1(t_i))(t_{i+1} - t_i) \quad (13)$$

Assume that the dike length is $2a_i$ at t_i and $2a_{i+1}$ at t_{i+1}. The cross-sectional area of a dike at t_i is

$$A_i = 2a_i\delta_{ave}^i = \frac{2(1-\nu^2)a_i^2K_{Ic}}{E\sqrt{\pi\, a_i}}\int_{-1}^{1}\left[\frac{1}{\widetilde{\psi}_i^{(0)}(1)}\int_{r}^{1}\frac{\widetilde{\psi}_i^{(0)}(s)}{\sqrt{1-s^2}}ds + \frac{1}{\widetilde{\psi}_i^{(1)}(1)}\int_{r}^{1}\frac{\widetilde{\psi}_i^{(1)}(s)}{\sqrt{1-s^2}}ds\right]dr \quad (14)$$

The cross-sectional area of the dike decreases during propagation because of magma solidification. The reduction in the cross-sectional area of the dike from t_i to t_{i+1} ($i > 1$) can be approximately evaluated from the change in the solidified area of magma

$$\frac{A_i - A_{i+1}}{2} = 2\lambda_i\sqrt{\kappa}\sqrt{t_{i+1} - t_i}\Delta d_{i+1} + \sum_{j=1}^{i-1} \cdot 2\lambda_i\sqrt{\kappa}\left(\sqrt{t_{j+1}} - \sqrt{t_j}\right)\Delta d_{i+1-j} + 2\lambda_i\sqrt{\kappa}\left(\sqrt{t_{i+1}} - \sqrt{t_i}\right)\left(a_i - \sum_{j=1}^{i}\Delta d_{i+2-j}\right) \quad (15a)$$

when

$$\sum_{j=1}^{i}\Delta d_j < 2a_i$$

and

$$\frac{A_i - A_{i+1}}{2} = 2\lambda_i\sqrt{\kappa}\sqrt{t_{i+1} - t_i}\Delta d_{i+1} + \sum_{j=1}^{i\max} 2\lambda_i\sqrt{\kappa} \cdot \left(\sqrt{t_{j+1}} - \sqrt{t_j}\right)\Delta d_{i+1-j} \quad (15b)$$

when

$$\sum_{j=1}^{i} \Delta d_j \geq 2a_i$$

where *i*max is the maximum integer such that

$$\sum_{j=1}^{i\max} \Delta d_j < 2a_i$$

The new dike length $2a_{i+1}$ can be approximately determined from the new area A_{i+1} using equation (14). The total dike propagation length d from t_0 (= 0) to t_{I+1} is thus given by

$$d = \sum_{i=0}^{I} \Delta d_i = \sum_{i=0}^{I} \frac{\left(\delta_{ave}^{i}\right)^2}{12\eta} \left(\Delta\rho g + \frac{K_{Ic}}{a_i \sqrt{\pi\, a_i}\, \widetilde{\psi}_i^{(1)}(1)} \right) \cdot (t_{i+1} - t_i) \tag{16}$$

The dike length also decreases with decreasing dike cross-sectional area during propagation. Dike propagation will stop if the velocity given by equation (9) becomes zero. This condition is expressed as

$$p_1 = -\frac{K_{Ic}}{a\sqrt{\pi\, a}\, \widetilde{\psi}^{(1)}(1)} = \Delta\rho g \tag{17}$$

The dikes thus cease to propagate if the length decreases to the following critical value

$$a_{cri} = \left(-\frac{K_{Ic}}{\Delta\rho g \sqrt{\pi}\widetilde{\psi}^{(1)}(1)} \right)^{2/3} \tag{18}$$

Dike propagation duration and distance then can be determined using equations (16) and (18). At the time of stalling, the dike still contains a significant volume of hot magma, which will then crystallize in situ, releasing volatiles into the mantle wedge [*Spera*, 1984].

3. Numerical Results

3.1. Introduction and General Assumptions

[24] This section presents numerical examples to illustrate the effects of magma solidus, magma viscosity, magma density and host rock fracture toughness on dike propagation distance and velocity. We also consider the effect of dike spacing in the case of multiple dikes. In all calculations, we use the following properties for typical basaltic magma and host rock [*Rubin*, 1995b]: E = 20 GPa, ν = 0.25, ρ_{mantle} = 3300 kg/m^3, and κ = 3 mm^2/s, c = 1.5 kJ/(kg K), L = 500 kJ/kg. The temperature dependence of material properties is not considered following most studies on dike propagation [e.g., *Spence et al.*, 1987; *Rubin*, 1995a, 1998]. The solution is thus of first-order approximation. In our parametric sensitivity studies, magma viscosity varies from 10 to 100 Pa s, magma solidus varies from 800 to 1100°C, and magma density varies from 2400 to 2700 kg/m^3.

[25] We also explore the sensitivity of dike propagation to the host rock fracture toughness with values varying from 50 to 300 MPa m$^{1/2}$. Fracture toughness represents a material's resistance to crack propagation. Fracture toughness of rocks under atmospheric pressure and room temperature conditions is on the order of 1 MPa m$^{1/2}$ [*Atkinson and Meredith*, 1987; *Scholz*, 2002]. Fracture toughness of mantle rocks under high confining pressures and high temperatures, however, may become significantly higher. Although fracture toughness data under mantle pressures and temperatures is not available, some experimental investigations on the fracture toughness of basalts [*Balme et al.*, 2004], limestone [*Schmidt and Huddle*, 1977; *Al-Shayea et al.*, 2000], and sandstone [*Winter*, 1983; *Terrien et al.*, 1983] have shown that fracture toughness increases with an increase in confining pressure. For example, *Schmidt and Huddle* [1977] showed that the toughness increases from 1 to 4.2 MPa m$^{1/2}$ when the confining pressure increases from 7 to 62 MPa. If the trend of fracture toughness with increasing confining pressure persists to 1.5 GPa, extrapolation of the test data of *Schmidt and Huddle* [1977] would give a fracture toughness on the order of 100 MPa m$^{1/2}$. For a Icelandic basalt, *Balme et al.* [2004] showed moderate fracture toughness increase with confining pressure and concluded that fracture toughness of igneous rocks may not reach 100 MPa m$^{1/2}$, a level suggested from dike propagation models [e.g., *Delaney and Pollard*, 1981; *Parfitt*, 1991, *Rivalta and Dahm*, 2006; *Jin and Johnson*, 2008a]. The basalt used by *Balme et al.* [2004], however, is a quenched rock and hence may be significantly more brittle than that under mantle temperatures. Under the mantle pressure and temperature conditions, viscous-plastic deformations are pronounced and dissipate significant energy during dike propagation in a way similar to that for metals. The effective fracture toughness thus may well reach the order of 100 MPa m$^{1/2}$, a value for typical ductile metals. Hence, we suggest that the range of toughness values considered in

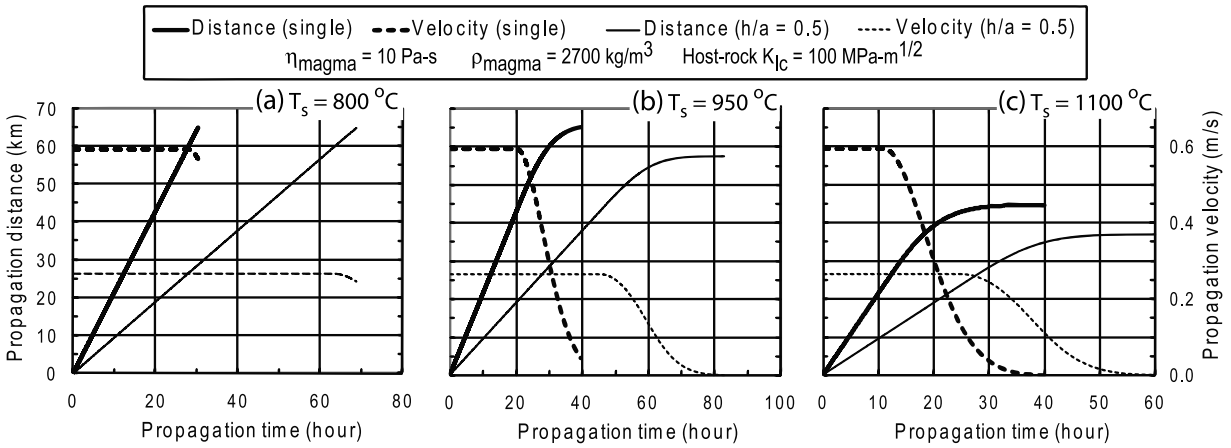

Figure 3. Dike propagation distance/velocity versus time (η = 10 Pa s, ρ_{magma} = 2700 kg/m^3, and K_{Ic} = 100 MPa m$^{1/2}$). (a) T_s = 800°C, (b) T_s = 950°C, and (c) T_s = 1100°C.

our sensitivity analysis may be appropriate for the upper part of the mantle wedge.

[26] We assume that dikes initiate in the thermal core of the mantle wedge at 100 km depth. In sections 3.2 and 3.3, we consider the thermal structure in Figure 1a, which represents a cooler mantle wedge. We consider the hotter mantle wedge of Figure 1b in section 3.4. The temperature gradient in the cooler mantle wedge of Figure 1a is approximately modeled by the following power function

$$T_0(Y) = 133.86Y^{0.487} \tag{19}$$

where Y is the depth in km. Equation (19) gives a local wedge temperature of about 1260°C at the initial dike location (100 km depth) and about 760°C at the Moho (35 km depth). In sections 3.2 and 3.3 we restrict our parametric analysis to dikes of 2 km length. We do this for two reasons: (1) 2 km is moderately larger than the critical dike lengths determined by equation (18) for single dikes in the parameter space considered (the critical lengths are 0.9 km and 1.87 km for K_{Ic} = 100 MPa m$^{1/2}$ and 300 MPa m$^{1/2}$, respectively, with ρ_{magma} = 2700 kg/m^3) and (2) we are interested in the transitional behavior between dikes that can make it to the Moho and those that cannot. *Rubin* [1998] has reported that a dike in partially molten mantle may grow to 5 km long by porous flow of melts from the host rock into the dike. Thus, we consider 2 km to be a reasonable, though perhaps conservative, length for our primary sensitivity analyses. In section 3.5 we show the effects of increasing dike length up to 5 km. The dike spacing for the multiple, parallel dikes is taken as h/a = 0.5 (i.e., 1 km spacing for 2 km long dikes).

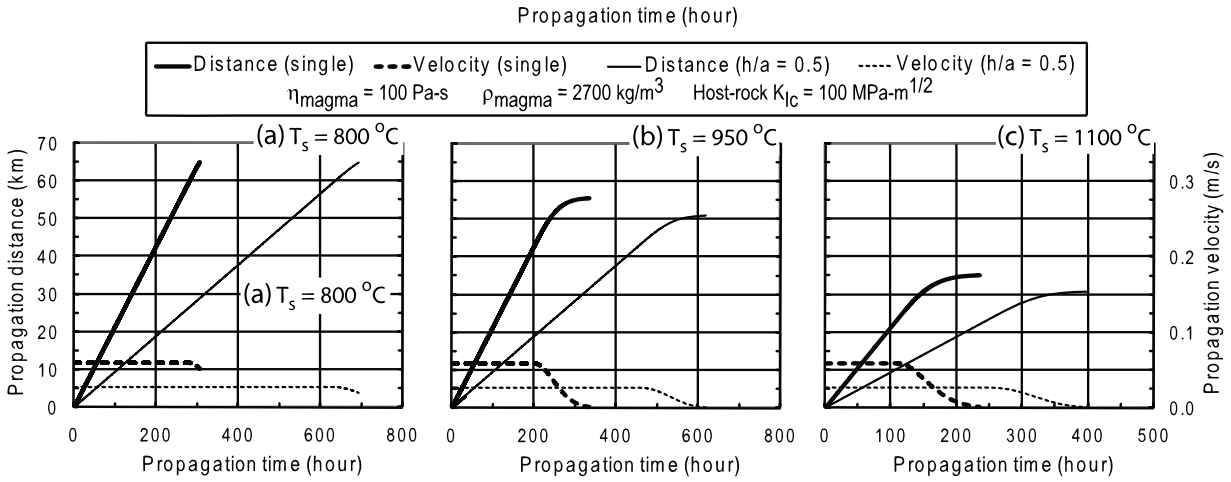

Figure 4. Dike propagation distance/velocity versus time (η = 100 Pa s, ρ_{magma} = 2700 kg/m^3, and K_{Ic} = 100 MPa m$^{1/2}$). (a) T_s = 800°C, (b) T_s = 950°C, and (c) T_s = 1100°C.

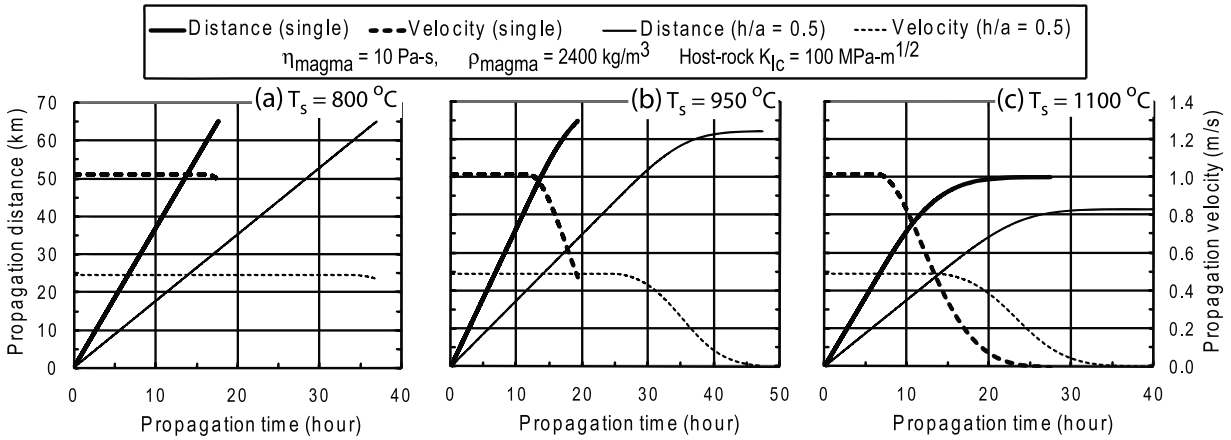

Figure 5. Dike propagation distance/velocity versus time (η = 10 Pa s, ρ_{magma} = 2400 kg/m^3, and K_{Ic} = 100 MPa m$^{1/2}$). (a) T_s = 800°C, (b) T_s = 950°C, and (c) T_s = 1100°C.

3.2. Propagation Distance Versus Time

[27] Figures 3–6 show dike propagation distances and velocities versus time for both a single dike and an array of parallel dikes. The fracture toughness of the host rock is assumed as 100 MPa m$^{1/2}$. The magma density is 2700 kg/m^3 in Figures 3 and 4, and 2400 kg/m^3 in Figures 5 and 6. The magma viscosity is 10 Pa s in Figures 3 and 5, and 100 Pa s in Figures 4 and 6.

[28] Figure 3a shows that when the magma solidus is 800°C, dikes traverse the mantle at constant velocity until they near the Moho, where a slight velocity decrease indicates marginal magma solidification. The dikes may or may not penetrate the Moho depending on whether or not the fracture toughness of the crustal rock is significantly lower than that of the mantle, and how rapidly the density decreases. For our purposes here we only present the results for dike propagation in the mantle, and will consider Moho penetration and propagation into the crust in a later analysis. Figure 3b shows that for an increased magma solidus of 950°C, a single dike can still reach the Moho without complete solidification although the propagation velocity decreases dramatically from a steady state value of 0.59 m/s to about 0.045 m/s as the dike reaches the Moho. The multiple dikes, however, can propagate only about 57 km and do not reach the Moho before the propagation velocity drops to zero. We note that the magma is not completely solidified when the dike stops propagating. Rather, propagation stops when the dike length becomes shorter than the critical length determined by equation (18). Figure 3c shows that no dikes can reach the Moho when the magma solidus is 1100°C.

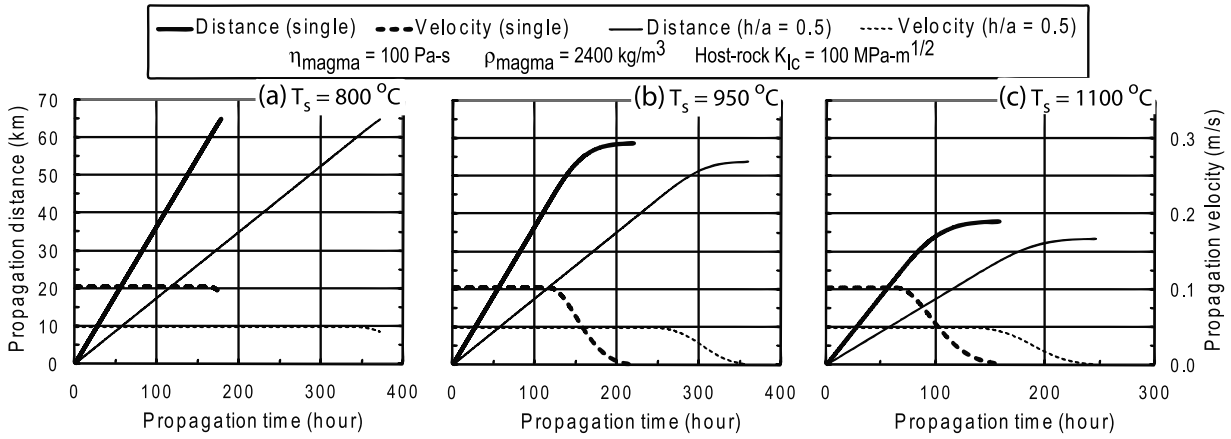

Figure 6. Dike propagation distance/velocity versus time (η = 100 Pa s, ρ_{magma} = 2400 kg/m^3, and K_{Ic} = 100 MPa m$^{1/2}$). (a) T_s = 800°C, (b) T_s = 950°C, and (c) T_s = 1100°C.

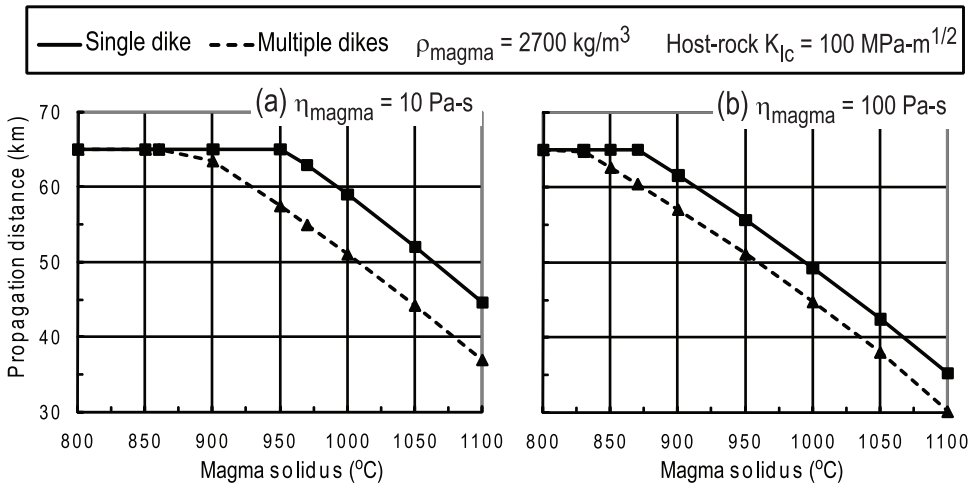

Figure 7. Effect of basalt solidus on the dike propagation distance (ρ_{magma} = 2700 kg/m^3 and K_{Ic} = 100 MPa m$^{1/2}$). (a) η = 10 Pa s and (b) η = 100 Pa s.

[29] Figure 4a shows that for an increased magma viscosity of 100 Pa s, both the multiple dikes and the single dike can reach the Moho when the magma solidus temperature is 800°C. The dike propagation velocities, however, are significantly lower compared with those for a magma viscosity of 10 Pa s (Figure 3a), which leads to much longer travel times. Figures 4b and 4c show that for an increased magma solidus of 950°C and 1100°C, no dikes of 2 km length can reach the Moho.

[30] Figures 5a–5c show similar dike propagation behavior to that in Figure 3, but with a reduced density of 2400 kg/m^3. Some dikes with solidus temperatures of 800 and 950°C can reach the Moho, but no dikes of 2 km length can reach the Moho when the solidus is 1100°C.

[31] Figures 6a–6c show similar dike propagation behavior to that in Figure 4, but with a reduced density of 2400 kg/m^3. Some dikes with solidus temperatures of 800°C can reach the Moho, but no dikes of 2 km length with this higher viscosity can reach the Moho for solidus temperatures of 950°C and 1100°C.

3.3. Physical Property Versus Propagation Distance

[32] Figures 7–11 summarize the effects of magma solidus temperature, magma viscosity, magma density and host rock fracture toughness, respectively, on dike propagation distance. The base parameters are as follows: magma viscosity of 10 Pa s (except Figure 8), magma density of 2700 kg/m^3 (except Figures 9 and 11), and fracture toughness of 100 MPa m$^{1/2}$ (except Figures 10 and 11).

[33] Figures 7a and 7b show the effect of magma solidus temperatures on the dike propagation distance. When the magma viscosity is 10 Pa s (Figure 7a), a single dike can reach the Moho when the solidus is less than 960°C, and multiple dikes can reach the Moho when the solidus is less than 870°C. Figure 7b shows that for an increased magma viscosity of 100 Pa s a single dike can reach the Moho when the solidus is less than 870°C, and the multiple dikes can reach the Moho when the solidus is less than 830°C.

[34] Figures 8a–8c show the effect of magma viscosity on the dike propagation distance. Single and multiple dikes can both reach the Moho in the range of viscosity considered when the magma solidus is 800°C (Figure 8a). Figure 8b shows that for an increased magma solidus of 950°C, only the single dike with a magma viscosity around 10 Pa s can propagate to the Moho. The propagation distance decreases with increasing magma viscosity but the decrease becomes modest as the viscosity approaches 100 Pa s. Figure 8c shows that when the magma solidus is 1100°C, no dikes can propagate to the Moho.

[35] Figures 9a–9c show the effect of magma density on the dike propagation distance. Single and multiple dikes can both propagate to the Moho over a magma density range of 2400 kg/m^3 to 2700 kg/m^3 when the magma solidus is 800°C (Figure 9a). Figure 9b shows that when the magma solidus is 950°C, the single dike can still propagate to the Moho in the magma density range considered. Figure 9c shows that no dikes can reach the Moho when the magma solidus is 1100°C. The

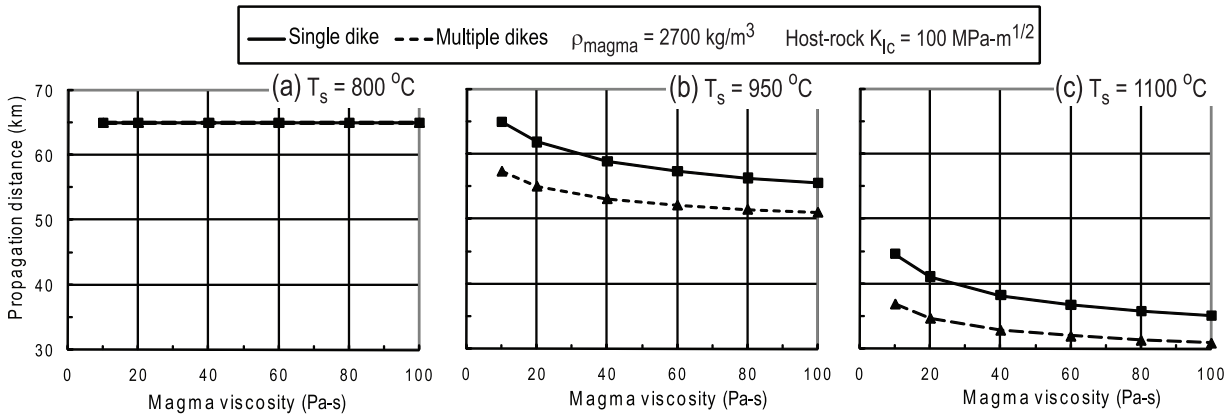

Figure 8. Effect of magma viscosity on the dike propagation distance (ρ_{magma} = 2700 kg/m^3 and K_{Ic} = 100 MPa m$^{1/2}$). (a) T_s = 800°C, (b) T_s = 950°C, and (c) T_s = 1100°C.

magma density does not influence the dike propagation distance as much as magma solidus or viscosity. For example, the propagation distance of the single dike decreases from 50 km to 45 km when the density increases from 2400 kg/m^3 to 2700 kg/m^3. For multiple dikes, the propagation distance decreases from 42 km to 37 km when the density increases from 2400 kg/m^3 to 2700 kg/m^3.

[36] Figures 10a–10c show the effect of fracture toughness of the host rock on the dike propagation distance for a magma density of 2700 kg/m^3. The single dike can propagate to the Moho over a toughness range of 50 MPa m$^{1/2}$ to 300 MPa m$^{1/2}$ when the magma solidus is 800°C (Figure 10a). The multiple dikes can also reach the Moho when the toughness is less than about 230 MPa m$^{1/2}$. The propagation distance of the multiple dikes, however, drops precipitously in the toughness range of 240 MPa m$^{1/2}$ to 243 MPa m$^{1/2}$ and the dikes do not propagate when the toughness exceeds about 243 MPa m$^{1/2}$. This is because the critical length of multiple dikes given in equation (18) is just above 2 km when the toughness is 243 MPa m$^{1/2}$. Figure 10b shows that for an increased magma solidus of 950°C, the single dike can propagate to the Moho when the fracture toughness is in the range of 90 MPa m$^{1/2}$ to 270 MPa m$^{1/2}$. The propagation distance decreases with increasing (decreasing) fracture toughness when the toughness is higher than 270 MPa m$^{1/2}$ (lower than 90 MPa m$^{1/2}$). For the multiple dikes, the propagation distance initially increases with increasing fracture toughness, reaches a peak value of about 58 km at a toughness of 130 MPa m$^{1/2}$, and then decreases with increasing fracture toughness. Generally speaking, dike propagation distance increases with an increase in host rock fracture toughness as a higher toughness yields a wider dike opening, which in turn requires a longer time for the magma to solidify. However, a higher toughness will result in a longer critical dike length (equation (18)) and

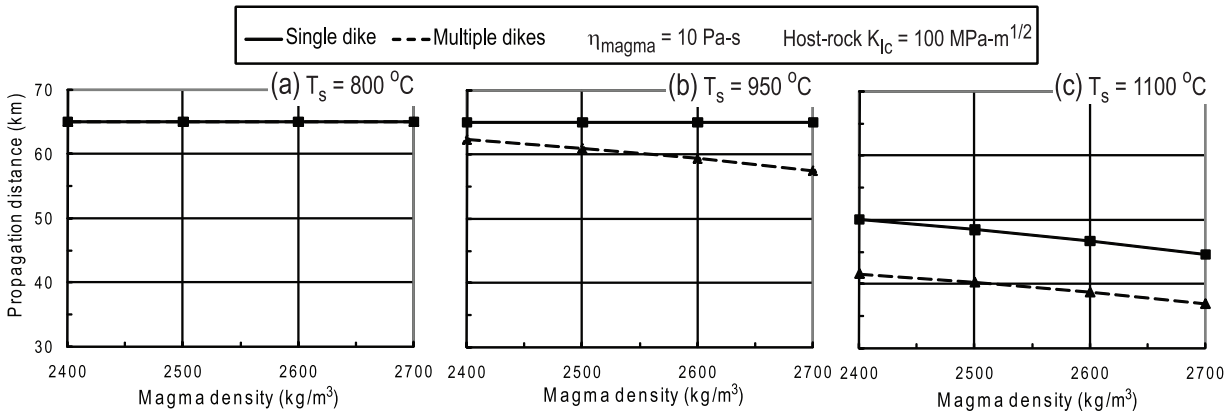

Figure 9. Effect of magma density on the dike propagation distance (η = 10 Pa s and K_{Ic} = 100 MPa m$^{1/2}$). (a) T_s = 800°C, (b) T_s = 950°C, and (c) T_s = 1100°C.

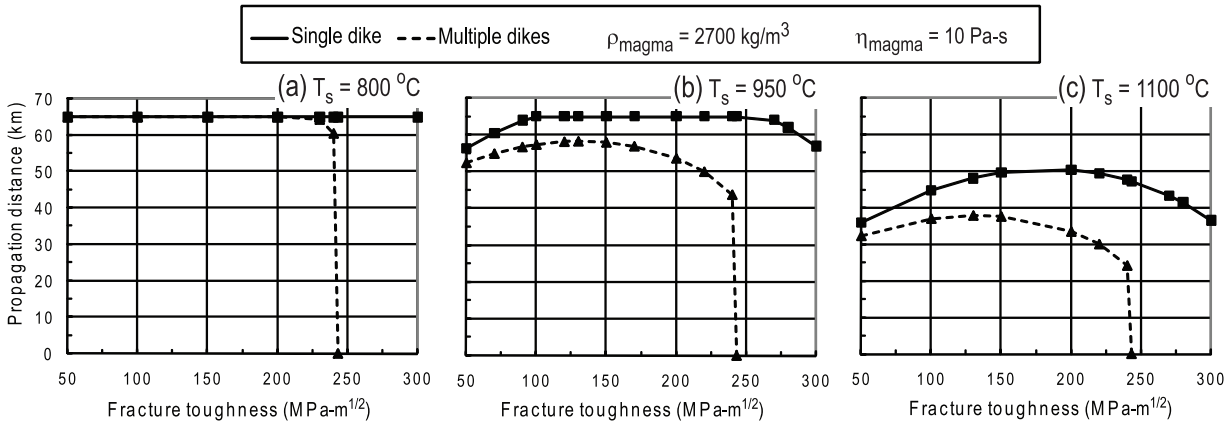

Figure 10. Effect of fracture toughness of host rock on the dike propagation distance (ρ_{magma} = 2700 kg/m^3 and η = 10 Pa s). (a) T_s = 800°C, (b) T_s = 950°C, and (c) T_s = 1100°C.

dike propagation distance will eventually decrease and drop to zero when the critical dike length approaches the actual dike length. Figure 10c shows that when the magma solidus is 1100°C, no dikes can reach the Moho. The propagation distance initially increases with increasing fracture toughness, reaches a peak of about 50 km for the single dike and about 38 km for the multiple dikes, and decreases with further increase in fracture toughness.

[37] Figures 11a–11c show the effect of fracture toughness of the host rock on the dike propagation distance for a reduced magma density of 2400 km/m^3. Figure 11a shows that both the single dike and multiple dikes can propagate to the Moho over a toughness range of 50 MPa m$^{1/2}$ to 300 MPa m$^{1/2}$ when the magma solidus is 800°C. This behavior for multiple dikes is different from that for a magma density of 2700 kg/m^3 shown in Figure 10a, because the critical dike length becomes shorter with a larger density contrast between the host rock and magma, and the dike velocity is still large enough for the dikes to propagate 65 km. Figure 11b shows that for an increased magma solidus of 950°C, the single dike can propagate to the Moho when the fracture toughness is in the range of 70 MPa m$^{1/2}$ to 300 MPa m$^{1/2}$. The multiple dikes can also reach the Moho when the toughness is in the range of 120 MPa m$^{1/2}$ to 270 MPa m$^{1/2}$, which contrasts with the result for a magma density of 2700 kg/m^3 shown in Figure 10b. Figure 11c shows that when the magma solidus further increases to 1100°C, the single dike can still propagate to the Moho when the toughness is in the range of 190 MPa m$^{1/2}$ to 300 MPa m$^{1/2}$ whereas no dikes can reach the Moho for a magma density of 2700 kg/m^3 shown in Figure 10c.

3.4. Role of the Mantle Wedge Thermal Structure on Propagation Distance

[38] The thermal structure that we have used for our primary analyses (Figure 1a) considers a man-

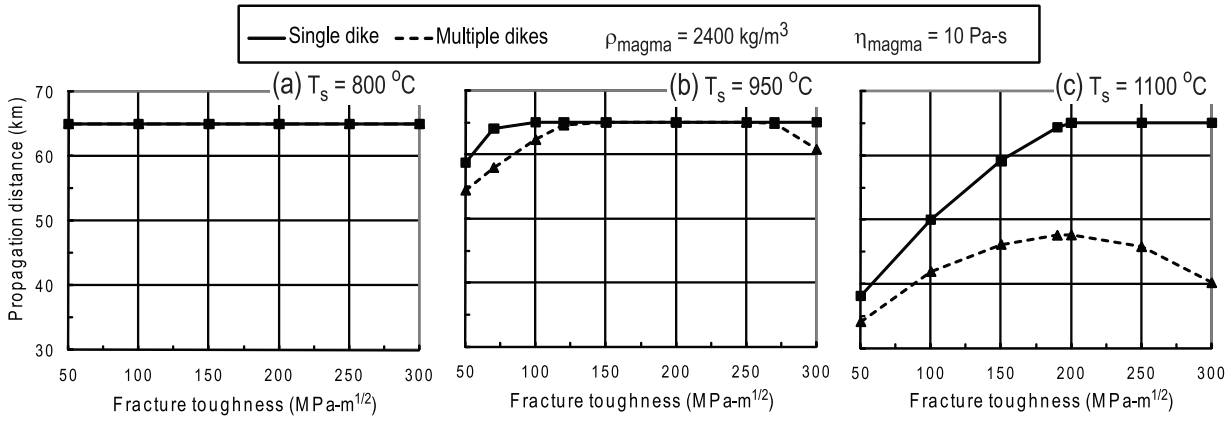

Figure 11. Effect of fracture toughness of host rock on the dike propagation distance (ρ_{magma} = 2400 kg/m^3 and η = 10 Pa s). (a) T_s = 800°C, (b) T_s = 950°C, and (c) T_s = 1100°C.

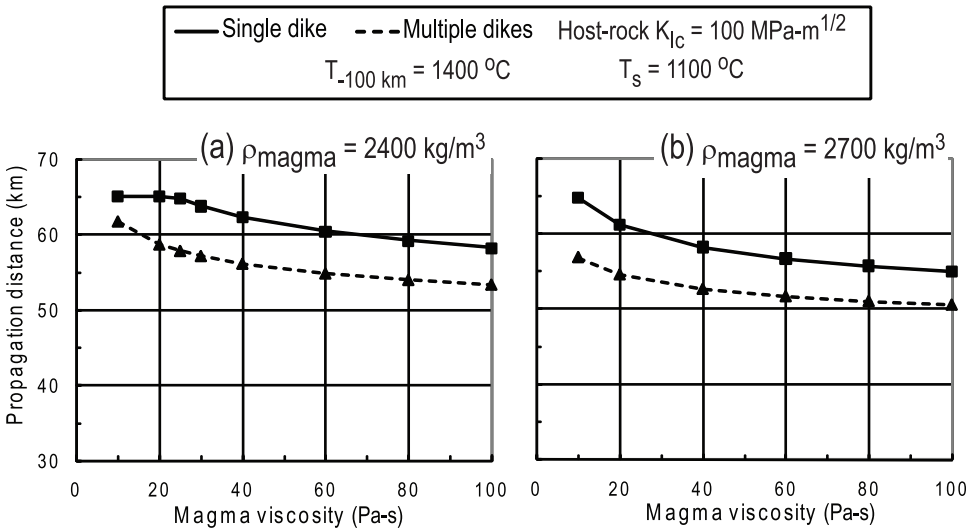

Figure 12. Effect of magma viscosity on the dike propagation distance: mantle with the thermal gradient of equation (20) (T_s = 1100°C and K_{Ic} = 100 MPa $m^{1/2}$). (a) ρ_{magma} = 2400 kg/m^3 and (b) ρ_{magma} = 2700 kg/m^3.

tle wedge that is significantly hotter than would be expected for an isoviscous linear mantle rheology. Nevertheless, our assumed thermal structure may be considered conservative in light of petrological constraints that suggest Moho temperatures significantly higher than 760°C (reviewed by *Kelemen et al.* [2003b]). In the numerical experiments presented above, magma with a solidus temperature of 1100°C was unable to make it to the Moho across almost our entire parameter space, except for a case of single dike propagation in a high toughness mantle with low magma viscosity and magma density (Figure 11c). In order to investigate the role of host rock temperature on propagation distance, we conducted additional numerical experiments for a magma solidus equal to 1100°C and a hotter thermal structure (Figure 1b) broadly similar to that modeled by *Furukawa* [1993], *van Keken et al.* [2002], *Kelemen et al.* [2003b], *Conder* [2005], *Manea et al.* [2005b], and *Peacock et al.* [2005]. To accomplish this, we assume a temperature gradient in the wedge that is approximately modeled by the following power function

$$T_0(Y) = 201.56Y^{0.421} \tag{20}$$

where Y is the depth in km. Equation (20) gives a local wedge temperature of about 1400°C at the initial dike location (100 km depth) and about 900°C at the Moho (35 km depth).

[39] Figures 12a and 12b show the effect of magma viscosity on dike propagation for fracture toughness of 100 MPa $m^{1/2}$ and solidus temperature of 1100°C. The single dike can propagate to the Moho when the viscosity is less than 25 Pa s for a magma density of 2400 kg/m^3 (Figure 12a). For an increased magma density of 2700 kg/m^3 the single dike can reach the Moho only if the viscosity reduces to 10 Pa s (Figure 12b). The multiple dikes, however, cannot reach the Moho in the range of viscosity and density considered.

[40] Figures 13a and 13b show the dike propagation distance versus fracture toughness for a magma viscosity of 10 Pa s and solidus temperature of 1100°C. The single dike propagates to the Moho when the toughness is higher than 75 MPa $m^{1/2}$ in the toughness range considered, and the multiple dikes reach the Moho when the toughness is higher than 130 MPa $m^{1/2}$ and lower than 270 MPa $m^{1/2}$ for a magma density of 2400 kg/m^3 (Figure 13a). For an increased magma density of 2700 kg/m^3, the single dike can reach the Moho when the toughness is in the range of 100 MPa $m^{1/2}$ to 260 MPa $m^{1/2}$ (Figure 13b). The multiple dikes, however, will not reach the Moho. The results in Figures 12 and 13 indicate that magmas with a solidus of 1100°C can be transported to the Moho through the propagation of 2-km-long dikes under a relative restricted range of conditions.

3.5. Role of Dike Length on Propagation Distance

[41] In the previous analyses we chose an initial dike length of 2 km, which is moderately larger than the critical dike lengths determined by equation (18) for

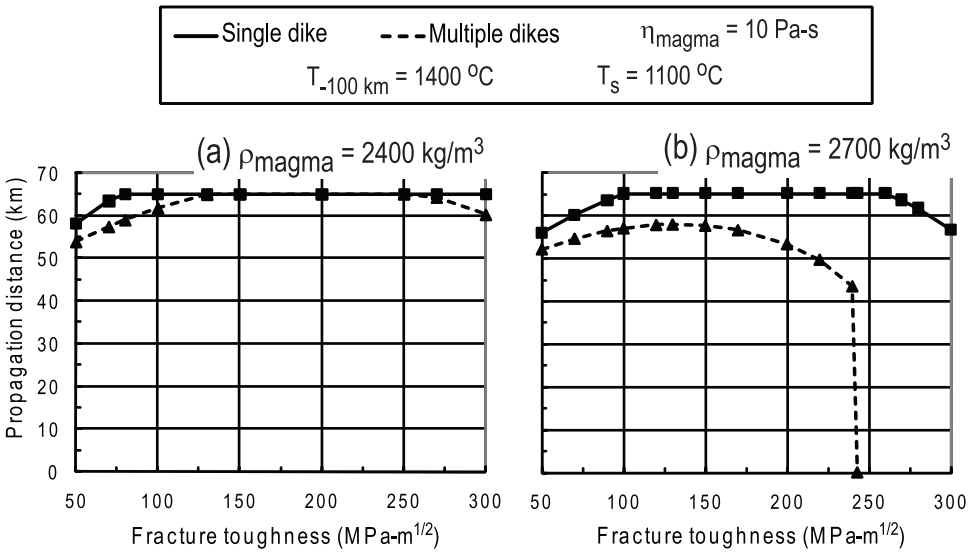

Figure 13. Effect of fracture toughness of host rock on the dike propagation distance: mantle with the thermal gradient of equation (20) (T_s = 1100°C and η = 10 Pa s). (a) ρ_{magma} = 2400 kg/m^3 and (b) ρ_{magma} = 2700 kg/m^3.

single dikes in the parameter space considered. Large igneous provinces, giant dike swarms, kimberlites, and basaltic lavas with very primitive compositions clearly show that magma propagation events from the mantle can be efficient and catastrophic, with large volumes of magma reaching Earth's surface [e.g., *Fialko and Rubin*, 1999; *Grégoire et al.*, 2006]. However, these are rare to extraordinary events, and we suggest that in general dikes will propagate at critical velocities once there is enough magma segregated to allow the dike to reach a length somewhat larger than its critical length. This sort of episodic, ballistic transport shows a self-organized behavior, and is likely to be important for transport of geological fluids in general [e.g., *Bons and van Milligen*, 2001].

[42] Nevertheless, the occurrence of primitive magma compositions [*Leat et al.*, 2002; *Kelemen et al.*, 2003a] in many modern and eroded arcs suggest that many dikes are large enough to carry hot magma directly from the source, well into the crust or even to its surface, without significant fractionation or contamination. As noted earlier, *Rubin* [1998] reported that a dike in partially molten mantle may grow to up to 5 km long by porous flow of melts from the host rock into the dike. Thus, here we briefly show sensitivity of dike propagation distance to its initial length, considering dikes that range in length from 2 to 5 km and both mantle thermal structures shown in Figure 1. We also restrict this part of our analysis to dikes containing magma with a solidus temperature of 1100°C, because (1) primitive arc magmas may commonly have temperatures >1100°C and we are interested in providing some constraints on their transport from the mantle to the crust and (2) this solidus temperature represents an end-member in our parameter space that provides bounding constraints on propagation distance versus dike length.

[43] Figures 14a and 14b show the dike propagation distance versus initial dike length for a fracture toughness of 100 MPa m$^{1/2}$, viscosity of 10 Pa s, a solidus temperature of 1100°C, and the more conservative thermal structure described by equation (19) and shown in Figure 1a. The magma densities are 2400 kg/m^3 and 2700 kg/m^3 in Figures 14a and 14b, respectively. As shown in Figure 14a, single dikes with lengths in the range of 3 to 5 km are able to transport magma from the core of the mantle wedge to the Moho. Multiple dikes can reach the Moho only when the initial lengths are greater than 4.5 km. Figure 14b shows that single dikes can make it to the Moho if the initial lengths are greater than 4 km and none of the multiple dikes can reach the Moho.

[44] Figures 15a and 15b show the dike propagation distance versus initial dike length for the hotter mantle with the thermal structure described by equation (20) and shown in Figure 1b. Other parameters are the same as those in Figures 14a and 14b. Under these conditions all single dikes in our parameter space can make it to the Moho. The multiple dikes initially longer than 2.3 km (for a magma density of 2400 kg/m^3 (Figure 15a)) or

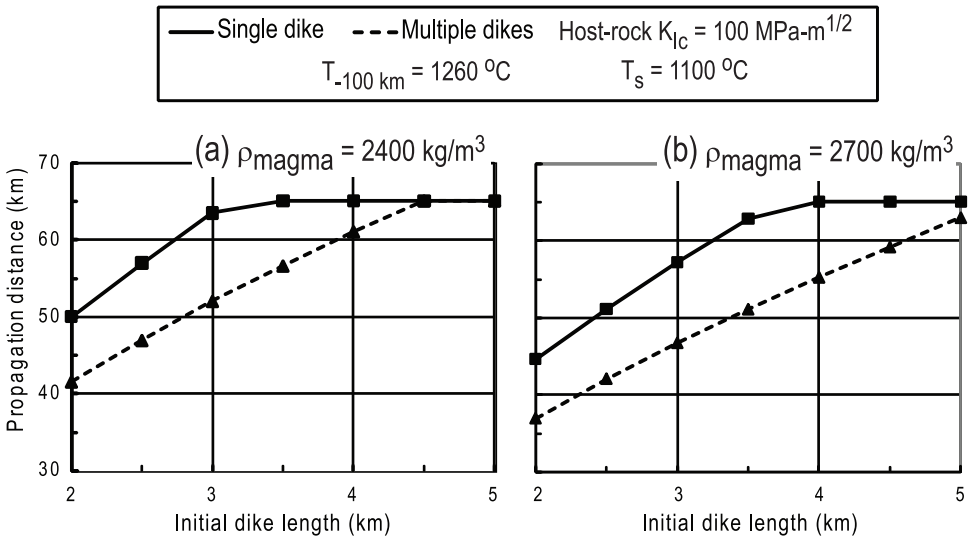

Figure 14. Dike propagation distance versus initial dike length: mantle with the thermal gradient of equation (19) (T_s = 1100°C, η = 10 Pa s, and K_{Ic} = 100 MPa $m^{1/2}$). (a) ρ_{magma} = 2400 kg/m^3 and (b) ρ_{magma} = 2700 kg/m^3.

2.7 km (for a magma density of 2700 kg/m^3 (Figure 15b)) can also propagate to the Moho.

4. Discussion

4.1. Primitive Basaltic Magma Transport to the Arc Crust

[45] Primitive basaltic arc magmas have Mg # > 60, are variably hydrous, and may commonly have temperatures >1100°C although this is uncertain for H_2O-rich compositions [*Kelemen et al.*, 2003a]. Although relatively rare in arcs, primitive magmas are petrologically important because they closely reflect the compositions of their mantle sources. They also provide important constraints on magma ascent processes because the primitive magma needs to get from its source to its sink without experiencing significant fractionation or contamination. We suggest that dikes are the only viable mechanism for primitive basaltic magma ascent through the crust, but this leaves open the question of whether dikes can extract primitive magmas from deep in the core of the mantle wedge, from which much of the melt in subduction zones is likely to be sourced.

[46] The results in our numerical analyses in section 3 show that many dikes of length 2–5 km

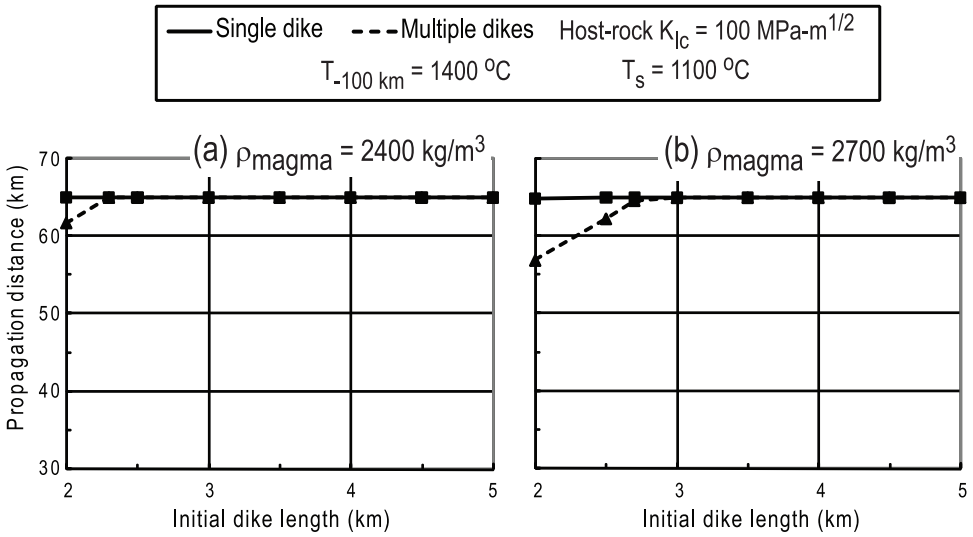

Figure 15. Dike propagation distance versus initial dike length: mantle with the thermal gradient of equation (20) (T_s = 1100°C, η = 10 Pa s, and K_{Ic} = 100 MPa $m^{1/2}$). (a) ρ_{magma} = 2400 kg/m^3 and (b) ρ_{magma} = 2700 kg/m^3.

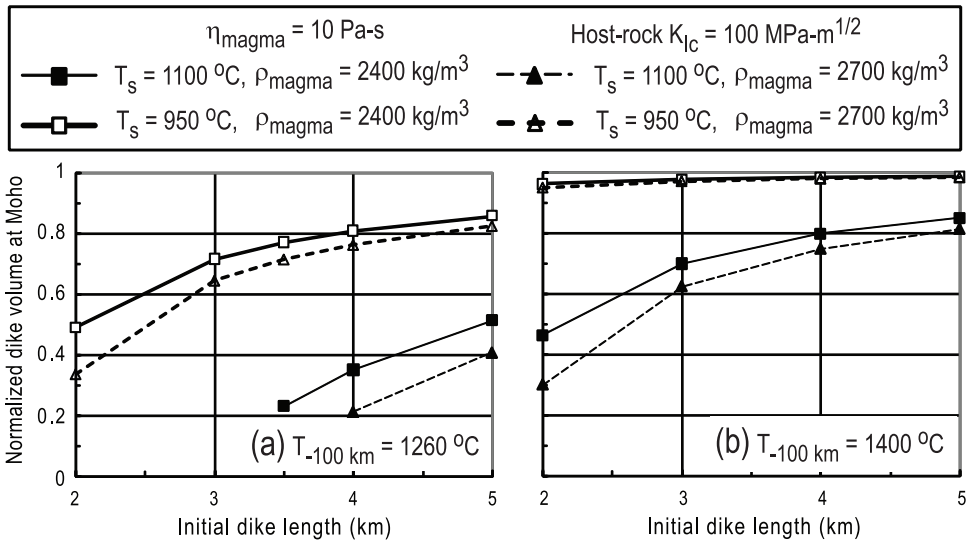

Figure 16. Volume of dike propagated to the Moho normalized by its original volume (η = 10 Pa s and K_{Ic} = 100 MPa $m^{1/2}$). (a) Mantle with the thermal gradient of equation (19) and (b) mantle with the thermal gradient of equation (20).

can propagate to the Moho, some with less than 2% solidification, depending strongly on the dike length and the mantle thermal structure. Figure 16 illustrates the effects of these two variables. Figure 16a shows the normalized dike volume (normalized by the initial dike volume) at the Moho versus the initial dike length for a fracture toughness of 100 MPa $m^{1/2}$, viscosity of 10 Pa s, and the more conservative thermal structure of equation (19) and Figure 1a. Solidus temperatures of 1100 and 950°C, and magma densities of 2400 and 2700 kg/m^3 are considered. Only single dikes are considered and dikes that cannot propagate to the Moho are excluded. The results show that dike volume at the Moho is below 51% of initial dike volume for a solidus of 1100°C, which indicates that the magma has undergone significant solidification. For a reduced solidus of 950°C, significant magma solidification also occurs for dikes with an initial length less than 3 km, with the 5 km dikes showing a volume reduction of less than 20%.

[47] Figure 16b shows the normalized dike volume at the Moho versus the initial dike length for the hotter mantle with the thermal structure of equation (20) and Figure 1b. Other parameters are the same as those in Figure 16a. For dikes with a solidus of 1100°C, significant magma solidification also occurs for dikes with an initial length less than 3 km, with the 5 km dikes showing a volume reduction of less than 20%. At these mantle temperatures, magma solidification is minimal for all dikes when the solidus is 950°C with the dike volumes at the Moho > 95% of their corresponding initial volume at 100 km depth. The 5 km dike experiences less than 2% volume reduction.

[48] It appears then that, given our parameter space, it is possible with relatively long dikes and hot mantle to extract primitive magmas from the wedge to the crust with minimal fractionation. Given an even hotter mantle [e.g., *Elkins-Tanton et al.*, 2001], it becomes possible to extract primitive magma from the wedge in all dikes of our parameter space. But then again, in such transiently hot mantle wedges in which the Moho temperature is very near the magma solidus temperature, dikes could extract primitive magmas from just a few km below the Moho, from zones of partial melt or, perhaps, off the top of stalled reaction infiltration fronts.

[49] An important limitation of the solidification model used in this work is that magma flow is not considered in equation (11), and so we probably overestimate the thickness of the solidified magma layer on dike walls by not accounting for viscous energy dissipation [e.g., *Spera*, 1980]. Moreover, our analysis assumes laminar flow in the dikes, but cross-stream flow of magma is expected because of dike wall roughness and other factors [*Spera*, 1980; *Carrigan et al.*, 1992]. These effects would significantly decrease volume loss of magma due to dike wall crystallization, consequently increasing the range of dikes within our parameter space that could transport primitive magmas to the crust.

Once these dikes reach the crust, they run the risk of encountering existing magma chambers, which has been suggested as one reason why primitive arc lavas are so rarely exposed in eroded crustal sections [*Leat et al.*, 2002].

4.2. Implications for Mantle Heterogeneity and Crustal Growth

[50] It is well accepted that the compositional heterogeneity of igneous rocks in the crust reflects, in part, compositional heterogeneity in the underlying mantle [e.g., *Leat et al.*, 2002; *Stern et al.*, 2006; *Cagnioncle et al.*, 2007]. What role might dikes play in developing mantle heterogeneity? Much of the magma generated in the continental crust, or entering it from below, never reaches the surface [e.g., *White et al.*, 2006], but instead becomes part of a large-scale material transfer or recycling process [e.g., *Paterson and Fowler*, 1993]. Similarly, much of the magma formed in the mantle wedge may never reach the Moho, or escape across it into the crust. Dikes, diapirs or reaction infiltration (porous flow) fronts that do not make it to the Moho will stall in the mantle wedge, and if they are still deep enough in the mantle they will become entrained in the corner flow and be recycled during hydrous melting at a later time. If these magmas contain appreciable volatile components, then these components may escape from the solidifying magma through hydrofractures, leading to mantle metasomatism [*Spera*, 1984, 1987]. Material detached from the base of the crust or the upper surface of the downgoing slab could enjoy a similar fate [e.g., *Hall and Kincaid*, 2001; *Jull and Kelemen*, 2001; *Gerya and Yuen*, 2003; *Elkins-Tanton*, 2005; *Manea et al.*, 2005a, 2005b], contributing to the heterogeneity observed in arc magma compositions.

[51] Although we show that many dikes are able to make it to and across the Moho, many others that begin to ascend close to their critical length will stall in the mantle wedge, or pond into lenticular magma bodies. We do not know how volumetrically significant these additions to the mantle are. Because our analysis assumes plane strain, our calculations do not provide constraints on the arc-parallel, y dimension of the dikes, so we are not able to calculate true volumes. To do so we would need to assume a particular three-dimensional state of stress, which is beyond the scope of this work. For the following discussion, we consider the y dimension to be equivalent to the characteristic in-plane dimension (dike length), and we use the same material properties as in Figure 16. Given these assumptions, a dike 2 km in length will have a volume of approximately 5×10^{-4} km^3. For sake of argument, if 100 km^3/km/Ma of crustal growth is attributed entirely to dikes then, given our various assumptions, approximately one dike of 2 km length would be required to reach and completely enter or drain into the crust every 5 years on average for every linear km of arc (>190300 dikes per Ma).

[52] It is unclear what melt volumes are to be expected in the mantle wedge. *Zellmer* [2008] showed that melt flux is proportional to convergence rate, and therefore to the rate of water added to the mantle wedge from the downgoing slab. The coupled models of *Cagnioncle et al.* [2007] suggest that a wide range of melt volumes can be generated, depending on how rapidly volatiles can migrate from the slab into the mantle wedge. *Cagnioncle et al.* [2007] assumed that fluids and melts migrate through porous flow; considering fluid migration into the wedge through self-propagating cracks [e.g., *Spera*, 1987] or focused flow in shear bands [e.g., *Katz et al.*, 2006; *Holtzman and Kohlstedt*, 2007] would significantly increase the interaction rates between fluids and solid peridotite, thus increasing the melting rate. Using the crust as an analog, it appears that ~20% of the magma that is generated within the crust, or enters it from below, reaches the surface [*White et al.*, 2006]. If similar proportions hold in the mantle, then the equivalent of an additional four dikes of 2 km length would stall in the mantle every 5 years per linear km of arc in order to achieve 100 km^3/km/Ma of crustal growth.

[53] In addition to deeply initiated dikes, some may initiate from much higher in the mantle. For example sub-Moho magma chambers can be built by dikes or reaction infiltration fronts that do not make it into the crust. Ponding of magmas near the Moho appears to occur in the vicinity of spreading ridges on the basis of seismic reflection data [e.g., *Nedimovic et al.*, 2005], and is also suggested in some arcs from seismic wave speed data [e.g., *Zhao and Hasegawa*, 1994; *Lees*, 2007; *Wiens et al.*, 2008]. Dikes may initiate at the interfaces between these chambers and the wall rocks in a process similar to that suggested by *Kelemen et al.* [1997] for mid-ocean ridges. A large unknown in any assessment of the volumetric contribution to the crust is the amount of lower crustal material that drips off into the mantle through viscous

delamination [*Jull and Kelemen*, 2001; *Elkins-Tanton*, 2005].

5. Summary and Conclusions

[54] In this paper we address (1) the conditions under which dikes can extract partial melts of the mantle at 100 km depth to the Moho at 35 km depth, (2) how fast this extraction can occur, and (3) how much magma volume is lost to crystallization en route. Using a coupled modeling framework that considers both single and multiple dikes, linear elastic fracture mechanics and magma solidification, we explore the sensitivity of dike propagation distance and velocity to magma solidus temperature, magma viscosity, magma density, host rock fracture toughness, dike length and mantle wedge thermal structure. As expected, lower magma viscosity and solidus lead to larger dike propagation velocity and distance, but interactions between mantle fracture toughness and magma density also greatly influence dike propagation behavior. In general, dike propagation distance increases with increasing fracture toughness and decreasing magma density because a higher toughness yields a wider dike opening, which in turn requires a longer time for the magma to solidify to the point where the dike length reaches the critical length and stalls. A lower magma density yields a higher buoyancy force and a higher dike propagation velocity. A higher toughness will result in a longer critical dike length, so for very high toughness values the dike length must increase significantly to be highly effective. If more than one dike is moving at any one time, their elastic interactions can reduce the dike openings, which results in lower dike propagation velocity and requires less time for the dikes to reduce to its critical length and stall.

[55] Dikes and reaction infiltration instabilities may be the only mechanisms of magma ascent from the mantle wedge in subduction zones that could possibly carry melt from its source to the crust without freezing, and in time periods required by disequilibrium data for Uranium series isotopes. This is particularly true for magmas with primitive compositions, which must get from their source to their sink with minimal fractionation or contamination. If the estimated average rate from slab dewatering to surface eruption of 1 km a^{-1} [*Turner et al.*, 2001; *Bourdon et al.*, 2003; *Peate and Hawkesworth*, 2005] is found to be robust, then dikes may be the primary mechanism of magma extraction from the mantle wedge above subduction zones, particularly in instances where the magma must cross a thermal boundary layer of significant thickness. Alternatively, dikes and porous flow may work together to facilitate magma extraction [e.g., *Rubin*, 1998; *Kelemen et al.*, 2003b]. Our numerical results suggest that in the ranges of physical properties of host rock and magma considered in the present study many dikes of 2 km length are likely to make it from a depth of 100 km in the mantle wedge to a Moho at 35 km depth in less than a few hundred hours. Increasing initial dike length to 5 km ensures that nearly all dikes in our parameter space make it to the Moho. This mechanism for the ascent of partial mantle melts easily satisfies the constraints provided by U series isotopic disequilibrium.

[56] Field observations show that some arc magmas, though rare, have primitive compositions presumably reflecting minimal fractionation or contamination from source to sink. Our numerical results show that partial mantle melts with solidi in the range of 950–1000°C can reach the Moho with relatively little volume loss (loss of 2–20%) for the two mantle thermal structures considered. However, magma with a solidus temperature of 1100°C can only make it to the Moho with less than 20% volume loss in the hotter mantle of equation (20) and Figure 1b. Our results suggest that, given our assumptions and parameter space, primitive magmas in arc settings require dikes larger than ~5 km or a mantle thermal structure in which the temperature at the Moho is around 950°C or higher. If some of our assumptions are relaxed, such as laminar flow of the magma, dikes could more efficiently transport magma to the Moho, and thus may not require such high Moho temperatures. We conclude that dike transport is a viable mechanism for extracting primitive magmas from a source at 100 km depth in the mantle wedge to the crust in timeframes required by disequilibrium data for Uranium series isotopes.

Acknowledgments

[57] This work was partly supported by National Science Foundation grants EAR-0440063 and EAR-0810039 and the American Chemical Society, Petroleum Research Fund, grant 47463-AC8. Two anonymous reviews led to improvements in the manuscript. Editor Peter van Keken is thanked for his editorial guidance.

References

Aharonov, E., J. A. Whitehead, P. B. Kelemen, and M. Spiegelman (1995), Channeling instability of upwelling melt in the mantle, *J. Geophys. Res.*, *100*, 20,433–20,450.

Al-Shayea, N. A., K. Khan, and S. N. Abduljauwad (2000), Effects of confining pressure and temperature on mixed-mode (I-II) fracture toughness of a limestone rock, *Int. J. Rock Mech. Min. Sci.*, *37*, 629–643, doi:10.1016/S1365-1609(00)00003-4.

Arculus, R. J. (1994), Aspects of magma genesis in arcs, *Lithos*, *33*, 189–208, doi:10.1016/0024-4937(94)90060-4.

Atkinson, B. K., and P. G. Meredith (1987), Experimental fracture mechanics data for rocks and minerals, in *Fracture Mechanics of Rock*, edited by B. K. Atkinson, pp. 477–525, Academic, London.

Bahr, H. A., G. Fischer, and H. J. Weiss (1986), Thermal shock crack patterns explained by single and multiple crack propagation, *J. Mater. Sci.*, *21*, 2716–2720, doi:10.1007/BF00551478.

Balme, M. R., V. Rocchi, C. Jones, P. R. Sammonds, P. G. Meredith, and S. Boon (2004), Fracture toughness measurements on igneous rocks using a high-pressure, high-temperature rock fracture mechanics cell, *J. Volcanol. Geotherm. Res.*, *132*, 159–172, doi:10.1016/S0377-0273(03)00343-3.

Bolchover, P., and J. R. Lister (1999), The effect of solidification on fluid-driven fracture, *Proc. R. Soc. London, Ser. A*, *455*, 2389–2409, doi:10.1098/rspa.1999.0409.

Bons, P. D., and B. P. van Milligen (2001), New experiment to model self-organized critical transport and accumulation of melt and hydrocarbons from their source rocks, *Geology*, *29*, 919–922, doi:10.1130/0091-7613(2001)029<0919:NETMSO>2.0.CO;2.

Bourdon, B., S. P. Turner, and A. Dosseto (2003), Dehydration and partial melting in subduction zones: Constraints from U-series disequilibria, *J. Geophys. Res.*, *108*(B6), 2291, doi:10.1029/2002JB001839.

Bruce, P. M., and H. E. Huppert (1990), Solidification and melting in dikes by the laminar flow of basaltic magma, in *Magma Transport and Storage*, edited by M. P. Ryan, pp. 87–101, John Wiley, Chichester, U. K.

Cagnioncle, A.-M., E. M. Parmentier, and L. T. Elkins-Tanton (2007), Effect of solid flow above a subducting slab on water distribution and melting at convergent plate boundaries, *J. Geophys. Res.*, *112*, B09402, doi:10.1029/2007JB004934.

Cameron, B. I., J. A. Walker, M. J. Carr, L. C. Patino, O. Matias, and M. D. Feigenson (2003), Flux versus decompression melting at stratovolcanoes in southeastern Guatemala, *J. Volcanol. Geotherm. Res.*, *119*, 21–50, doi:10.1016/S0377-0273(02)00304-9.

Canon-Tapia, E., and O. Merle (2006), Dyke nucleation and early growth from pressurized magma chambers: Insights from analogue models, *J. Volcanol. Geotherm. Res.*, *158*, 207–220, doi:10.1016/j.jvolgeores.2006.05.003.

Carmichael, I. S. E., J. Nicholls, F. J. Spera, B. J. Wood, S. A. Nelson, D. K. Bailey, J. V. Smith, and M. J. O'Hara (1977), High-temperature properties of silicate liquids: Applications to the equilibration and ascent of basic magma, *Philos. Trans. R. Soc. London, Ser. A*, *286*, 373–431, doi:10.1098/rsta.1977.0124.

Carrigan, C. R., G. Schubert, and J. C. Eichelberger (1992), Thermal and dynamical regimes of single- and two-phase magmatic flow in dikes, *J. Geophys. Res.*, *97*, 17,377–17,392, doi:10.1029/92JB01244.

Conder, J. A. (2005), A case for hot slab surface temperatures in numerical viscous flow models of subduction zones with an improved fault zone parameterization, *Phys. Earth Planet. Inter.*, *149*, 155–164, doi:10.1016/j.pepi.2004.08.018.

Dahm, T. (2000a), Numerical simulations of the propagation path and the arrest of fluid-filled fractures in the earth, *Geophys. J. Int.*, *141*, 623–638, doi:10.1046/j.1365-246x.2000.00102.x.

Dahm, T. (2000b), On the shape and velocity of fluid-filled fractures in the earth, *Geophys. J. Int.*, *142*, 181–192, doi:10.1046/j.1365-246x.2000.00148.x.

Davies, J. H., and M. J. Bickle (1991), A physical model for the volume and composition of melt produced by hydrous fluxing above subduction zones, *Philos. Trans. R. Soc. London, Ser. A*, *335*, 355–364, doi:10.1098/rsta.1991.0051.

Davies, J. H., and D. J. Stevenson (1992), Physical model of source region of subduction zone volcanics, *J. Geophys. Res.*, *97*, 2037–2070, doi:10.1029/91JB02571.

Delaney, P. T., and D. D. Pollard (1981), Deformation of host rocks and flow of magma during growth of minette dikes and Breccia-bearing intrusions near Ship Rock, New Mexico, *U.S. Geol. Surv. Prof. Pap.*, *1202*, 61 pp.

Delaney, P. T., and D. D. Pollard (1982), Solidification of basaltic magma during flow in a dike, *Am. J. Sci.*, *282*, 856–885.

Dimalanta, C., A. Taira, G. P. Yumul Jr., H. Tokuyama, and K. Mochizuki (2002), New rates of western Pacific island arc magmatism from seismic and gravity data, *Earth Planet. Sci. Lett.*, *202*, 105–115, doi:10.1016/S0012-821X(02)00761-6.

Dufek, J., and G. W. Bergantz (2005), Lower crustal magma genesis and preservation: A stochastic framework for the evaluation of basalt-crust interaction, *J. Petrol.*, *46*, 2167–2195, doi:10.1093/petrology/egi049.

Eberle, M. A., O. Grasset, and C. Sotin (2002), A numerical study of the interaction between the mantle wedge, subducting slab, and overriding plate, *Phys. Earth Planet. Inter.*, *134*, 191–202, doi:10.1016/S0031-9201(02)00157-7.

Elkins-Tanton, L. T. (2005), Continental magmatism caused by lithospheric delamination, in *Plates, Plumes, and Paradigms*, edited by G. R. Foulger et al., *Spec. Pap. Geol. Soc. Am.*, *388*, 449–461, doi:10.1130/2005.2388(27).

Elkins-Tanton, L. T., T. L. Grove, and J. Donnelly Nolan (2001), Hot, shallow mantle melting under the Cascades volcanic arc, *Geology*, *29*, 631–634, doi:10.1130/0091-7613(2001)029<0631:HSMMUT>2.0.CO;2.

Fialko, Y. A., and A. M. Rubin (1998), Thermodynamics of lateral dike propagation: Implications for crustal accretion at slow spreading mid-ocean ridges, *J. Geophys. Res.*, *103*, 2501–2514, doi:10.1029/97JB03105.

Fialko, Y. A., and A. M. Rubin (1999), Thermal and mechanical aspects of magma emplacement in giant dike swarms, *J. Geophys. Res.*, *104*, 23,033–23,049, doi:10.1029/1999JB900213.

Furukawa, Y. (1993), Depth of the decoupling plate interface and thermal structure under arcs, *J. Geophys. Res.*, *98*, 20,005–20,013, doi:10.1029/93JB02020.

Gaetani, G. A., and T. L. Grove (2003), Experimental constraints on melt generation in the mantle wedge, in *Inside the Subduction Factory*, *Geophys. Monogr. Ser.*, vol. 138, edited by J. Eiler, pp. 107–134, AGU, Washington, DC.

Gerya, T. V., and D. A. Yuen (2003), Rayleigh-Taylor instabilities from hydration and melting propel "cold plumes" at subduction zones, *Earth Planet. Sci. Lett.*, *212*, 47–62, doi:10.1016/S0012-821X(03)00265-6.

Gill, J. B. (1981), *Orogenic Andesites and Plate Tectonics*, 390 pp., Springer, New York.

Grégoire, M., M. Rabinowicz, and A. J. A. Janse (2006), Mantle mush compaction: A key to understand the mechanisms of concentration of kimberlite melts and initiation of swarms of kimberlite dykes, *J. Petrol.*, *47*, 631–646, doi:10.1093/petrology/egi090.

Grove, T. L., N. Chatterjee, S. W. Parman, and E. Médard (2006), The influence of H_2O on mantle wedge melting, *Earth Planet. Sci. Lett.*, *249*, 74–89, doi:10.1016/j.epsl.2006.06.043.

Gupta, T. K. (1972), Strength degradation and crack propagation in thermally shocked Al_2O_3, *J. Am. Ceram. Soc.*, *55*, 249–253, doi:10.1111/j.1151-2916.1972.tb11273.x.

Hall, P., and C. Kincaid (2001), Diapiric flow at subduction zones: A recipe for rapid transport, *Science*, *292*, 2472–2475, doi:10.1126/science.1060488.

Holtzman, B. K., and D. L. Kohlstedt (2007), Stress-driven melt segregation and strain partitioning in partially molten rocks: Effects of stress and strain, *J. Petrol.*, *48*, 2379–2406, doi:10.1093/petrology/egm065.

Ito, G., and S. J. Martel (2002), Focusing of magma in the upper mantle through dike interaction, *J. Geophys. Res.*, *107*(B10), 2223, doi:10.1029/2001JB000251.

Jin, Z.-H., and S. E. Johnson (2008a), Magma-driven multiple dike propagation and fracture toughness of crustal rocks, *J. Geophys. Res.*, *113*, B03206, doi:10.1029/2006JB004761.

Jin, Z.-H., and S. E. Johnson (2008b), Primary oil migration through buoyancy–driven multiple fracture propagation: Oil velocity and flux, *Geophys. Res. Lett.*, *35*, L09303, doi:10.1029/2008GL033645.

Jull, M., and P. B. Kelemen (2001), On the conditions for lower crustal convective instability, *J. Geophys. Res.*, *106*, 6423–6446, doi:10.1029/2000JB900357.

Katz, R. F., M. Spiegelman, and B. Holtzman (2006), The dynamics of melt and shear localization in partially molten aggregates, *Nature*, *442*, 676–679, doi:10.1038/nature05039.

Kelemen, P. B., G. Hirth, N. Shimizu, M. Spiegelman, and H. J. B. Dick (1997), A review of melt migration processes in the adiabatically upwelling mantle beneath oceanic spreading ridges, *Philos. Trans. R. Soc. London, Ser. A*, *355*, 283–318, doi:10.1098/rsta.1997.0010.

Kelemen, P. B., K. Hanghoj, and A. R. Greene (2003a), One view of the geochemistry of subduction-related magmatic arcs, with an emphasis on primitive andesites and lower crust, in *The Crust*, *Treatise on Geochem.*, vol. 3, edited by R. L. Rudnick, pp. 593–659, Elsevier, Amsterdam.

Kelemen, P. B., J. L. Rilling, E. M. Parmentier, L. Mehl, and B. R. Hacker (2003b), Thermal structure due to solid-state flow in the mantle wedge beneath arcs, in *Inside the Subduction Factory*, *Geophys. Monogr. Ser.*, vol. 138, edited by J. Eiler, pp. 293–311, AGU, Washington, D. C.

Kuhn, D., and T. Dahm (2004), Simulation of magma ascent by dykes in the mantle beneath mid-ocean ridges, *J. Geodyn.*, *38*, 147–159, doi:10.1016/j.jog.2004.06.002.

Kushiro, I. (1990), Partial melting of mantle wedge and evolution of island arc crust, *J. Geophys. Res.*, *95*, 15,929–15,939, doi:10.1029/JB095iB10p15929.

Leat, P. T., T. R. Riley, C. D. Wareham, I. L. Millar, S. P. Kelley, and B. C. Storey (2002), Tectonic setting of primitive magmas in volcanic arcs: An example from the Antarctic Peninsula, *J. Geol. Soc.*, *159*, 31–44, doi:10.1144/0016-764900-132.

Lees, J. M. (2007), Seismic tomography of magmatic systems, *J. Volcanol. Geotherm. Res.*, *167*, 37–56, doi:10.1016/j.jvolgeores.2007.06.008.

Lister, J. R. (1994a), The solidification of buoyancy-driven flow in a flexible-walled channel. Part 1. Constant-volume release, *J. Fluid Mech.*, *272*, 21–44, doi:10.1017/S0022112094004362.

Lister, J. R. (1994b), The solidification of buoyancy-driven flow in a flexible-walled channel. Part 2. Continual release, *J. Fluid Mech.*, *272*, 45–65, doi:10.1017/S0022112094004374.

Lister, J. R., and P. J. Dellar (1996), Solidification of pressure-driven flow in a finite rigid channel with application to volcaniceruptions, *J. Fluid Mech.*, *323*, 267–283, doi:10.1017/S0022112096000912.

Lister, J. R., and R. C. Kerr (1991), Fluid-mechanical models of crack propagation and their application to magma transport in dikes, *J. Geophys. Res.*, *96*, 10,049–10,077, doi:10.1029/91JB00600.

Liu, J., S. R. Bohlen, and W. G. Ernst (1996), Stability of hydrous phases in subducting oceanic crust, *Earth Planet. Sci. Lett.*, *143*, 161–171, doi:10.1016/0012-821X(96)00130-6.

Manea, V. C., M. Manea, V. Kostoglodov, and G. S. Sewell (2005a), Thermo-mechanical model of the mantle wedge in the central Mexican subduction zone and a blob tracing approach for magma transport, *Phys. Earth Planet. Inter.*, *149*, 165–186, doi:10.1016/j.pepi.2004.08.024.

Manea, V. C., M. Manea, V. Kostoglodov, and G. Sewell (2005b), Thermal models, magma transport and velocity anomaly estimation beneath southern Kamchatka, in *Plates, Plumes, and Paradigms*, edited by G. R. Foulger et al., *Spec. Pap. Geol. Soc. Am.*, *388*, 517–536.

Nedimovic, M. R., S. M. Carbotte, A. J. Harding, R. S. Detrick, J. P. Canales, J. B. Diebold, G. M. Kent, M. Tischer, and J. M. Babcock (2005), Frozen magma lenses below the oceanic crust, *Nature*, *436*, 1149–1152, doi:10.1038/nature03944.

Nicolas, A. (1990), Melt extraction from mantle peridotites: Hydrofracturing and porous flow, with consequences for oceanic ridge activity, in *Magma Transport and Storage*, edited by M. P. Ryan, pp. 159–174, John Wiley, New York.

Nunn, J. (1996), Buoyancy-driven propagation of isolated fluid-filled fractures: Implications for fluid transport in Gulf of Mexico geopressured sediments, *J. Geophys. Res.*, *101*, 2963–2970, doi:10.1029/95JB03210.

Parfitt, E. A. (1991), The role of rift zone storage in controlling the site and timing of eruptions and intrusions at Kilauea Volcano, Hawaii, *J. Geophys. Res.*, *96*, 10,101–10,112, doi:10.1029/89JB03559.

Paterson, S. R., and T. K. Fowler (1993), Reexamining pluton emplacement processes, *J. Struct. Geol.*, *15*, 191–206, doi:10.1016/0191-8141(93)90095-R.

Peacock, S. M., P. E. van Keken, S. D. Holloway, B. R. Hacker, G. Abers, and R. L. Fergason (2005), Thermal structure of the Costa Rica–Nicaragua subduction zone: Slab metamorphism, seismicity and arc magmatism, *Phys. Earth Planet. Inter.*, *149*, 187–200, doi:10.1016/j.pepi.2004.08.030.

Pearce, J. A., and I. J. Parkinson (1993), Trace element models for mantle melting: Application to volcanic arc petrogenesis, *Geol. Soc. Spec. Publ.*, *76*, 373–403, doi:10.1144/GSL.SP.1993.076.01.19.

Peate, D. W., and C. J. Hawkesworth (2005), U-series disequilibria: Insights into mantle melting and the time scales of magma differentiation, *Rev. Geophys.*, *43*, RG1003, doi:10.1029/2004RG000154.

Plank, T., and C. H. Langmuir (1988), An evaluation of the global variations in the major element chemistry of arc basalts, *Earth Planet. Sci. Lett.*, *90*, 349–370.

Rivalta, E., and T. Dahm (2006), Acceleration of buoyancy-driven fractures and magmatic dikes beneath the free surface, *Geophys. J. Int.*, *166*, 1424–1439, doi:10.1111/j.1365-246X.2006.02962.x.

Rubin, A. M. (1995a), Propagation of magma-filled cracks, *Annu. Rev. Earth Planet. Sci.*, *23*, 287–336, doi:10.1146/annurev.ea.23.050195.001443.

Rubin, A. M. (1995b), Getting granite dikes out of the source region, *J. Geophys. Res.*, *100*, 5911–5929, doi:10.1029/94JB02942.

Rubin, A. M. (1998), Dike ascent in partially molten rock, *J. Geophys. Res.*, *103*, 20,901–20,919, doi:10.1029/98JB01349.

Schmidt, M. W., and S. Poli (1998), Experimentally based water budgets for dehydrating slabs and consequences for arc magma generation, *Earth Planet. Sci. Lett.*, *163*, 361–379, doi:10.1016/S0012-821X(98)00142-3.

Schmidt, M. W., and S. Poli (2003), Generation of mobile components during subduction of oceanic crust, in *The Crust*, *Treatise on Geochem.*, vol. 3, edited by R. L. Rudnick, pp. 567–591, Elsevier, Amsterdam.

Schmidt, R. A., and C. W. Huddle (1977), Effect of confining pressure on fracture toughness of Indiana limestone, *Int. J. Rock Mech. Min. Sci.*, *14*, 289–293, doi:10.1016/0148-9062(77)90740-9.

Scholz, C. H. (2002), *The Mechanics of Earthquakes and Faulting*, 2nd ed., Cambridge Univ. Press, Cambridge, UK.

Sisson, T. W., and S. Bronto (1998), Evidence for pressure release melting beneath magmatic arcs from basalt at Galungung, Indonesia, *Nature*, *391*, 883–886, doi:10.1038/36087.

Spence, D. A., P. Sharp, and D. L. Turcotte (1987), Buoyancy-driven crack propagation: A mechanism for magma migration, *J. Fluid Mech.*, *174*, 135–153, doi:10.1017/S0022112087000077.

Spera, F. J. (1980), Aspects of magma transport, in *Physics of Magmatic Processes*, edited by R. B. Hargraves, pp. 232–265, Princeton Univ. Press, Princeton, N. J.

Spera, F. J. (1984), Carbon dioxide in petrogenesis: III. Role of volatiles in the ascent of alkaline magma with special reference to xenolith-bearing mafic lavas, *Contrib. Mineral. Petrol.*, *88*, 217–232, doi:10.1007/BF00380167.

Spera, F. J. (1987), Dynamics of translithospheric migration of metasomatic fluid and alkaline magma, in *Mantle Metasomatism*, edited by M. A. Menzies and C. J. Hawkesworth, pp. 1–20, Academic, London.

Spera, F. J. (2000), Physical properties of magma, in *Encyclopedia of Volcanoes*, edited by H. Sigurdsson, pp. 171–190, Academic, San Diego, Calif.

Spiegelman, M., and P. B. Kelemen (2003), Extreme chemical variability as a consequence of channelized melt transport, *Geochem. Geophys. Geosyst.*, *4*(7), 1055, doi:10.1029/2002GC000336.

Stern, R. J., E. Kohut, S. H. Bloomer, M. Leybourne, M. Fouch, and J. Vervoort (2006), Subduction factory processes beneath the Guguan cross-chain, Mariana Arc: No role for sediments, are serpentinites important?, *Contrib. Mineral. Petrol.*, *151*, 202–221, doi:10.1007/s00410-005-0055-2.

Stracke, A., B. Bourdon, and D. McKenzie (2006), Melt extraction in the Earth's mantle: Constraints from U-Th-Pa-Ra studies in oceanic basalts, *Earth Planet. Sci. Lett.*, *244*, 97–112, doi:10.1016/j.epsl.2006.01.057.

Takada, A. (1994), Accumulation of magma in space and time by crack interaction, in *Magmatic Systems*, edited by M. P. Ryan, pp. 241–257, Academic, San Diego, Calif.

Tatsumi, Y. (1989), Migration of fluid phases and genesis of basalt magmas in subduction zones, *J. Geophys. Res.*, *94*, 4697–4707, doi:10.1029/JB094iB04p04697.

Terrien, M., J. P. Sarda, M. Chayed'Albissin, and J. Berges (1983), Experimental study of the anisotropy of a sandstone and a marble, paper presented at International Congress CNRS 351: Failure Criteria of Structured Media, Cent. Natl. de la Rech. Sci., Villard le Lans, France.

Turcotte, D. L., and G. Schubert (2002), *Geodynamics*, Cambridge Univ. Press, Cambridge, U. K.

Turner, S. P., R. M. M. George, P. J. Evans, C. J. Hawkesworth, and G. F. Zellmer (2000), Time scales of magma formation, ascent and storage beneath subduction-zone volcanoes, *Philos. Trans. R. Soc. London, Ser. A*, *358*, 1443–1464, doi:10.1098/rsta.2000.0598.

Turner, S. P., P. J. Evans, and C. Hawkesworth (2001), Ultrafast source-to-surface movement of melt at island arcs from ^{226}Ra-^{230}Th systematic, *Science*, *292*, 1363–1366, doi:10.1126/science.1059904.

Turner, S. P., B. Bourdon, and J. B. Gill (2003), Insights into magma genesis at convergent margins from U-series isotopes, in *Uranium-Series Geochemistry*, *Rev. in Mineral. and Geochem.*, vol. 52, edited by B. Bourdon et al., pp. 255–315, Mineral. Soc. of Am., Washington, D. C.

van Keken, P. E., B. Kiefer, and S. M. Peacock (2002), High-resolution models of subduction zones: Implications for mineral dehydration reactions and the transport of water into the deep mantle, *Geochem. Geophys. Geosyst.*, *3*(10), 1056, doi:10.1029/2001GC000256.

Weertman, J. (1971), Theory of water-filled crevasses in glaciers applied to vertical magma transport beneath oceanic ridges, *J. Geophys. Res.*, *76*, 1171–1183, doi:10.1029/JB076i005p01171.

White, S. M., J. A. Crisp, and F. J. Spera (2006), Long-term volumetric eruption rates and magma budgets, *Geochem. Geophys. Geosyst.*, *7*, Q03010, doi:10.1029/2005GC001002.

Wiens, D. A., J. A. Conder, and U. H. Faul (2008), The seismic structure and dynamics of the mantle wedge, *Annu. Rev. Earth Planet. Sci.*, *36*, 421–455, doi:10.1146/annurev.earth.33.092203.122633.

Winter, R. (1983), Bruchmechanische Gesteinsuntersuchungen mit dem Bezug zu hydraulischen Frac-Versuchen in Tiefbohrungen, dissertation, 179 pp., Ruhr-Univ. Bochum, Bochum, Germany.

Zellmer, G. F. (2008), Some first-order observations on magma transfer from mantle wedge to upper crust at volcanic arcs, in *Dynamics of Crustal Magma Transfer, Storage and Differentiation*, edited by C. Annen and G. F. Zellmer, *Geol. Soc. Spec. Publ.*, *304*, 15–31.

Zhao, D., and A. Hasegawa (1994), Teleseismic evidence for lateral heterogeneities in the northeastern Japan arc, *Tectonophysics*, *237*, 189–199, doi:10.1016/0040-1951(94)90254-2.